# Estimating Energy Efficiency of Connected and Autonomous Vehicles in a Mixed Fleet

## Final Report
## May 2018

ctre
Center for Transportation
Research and Education

**Sponsored by**
Iowa Highway Research Board
(IHRB Project TR-708D)
Midwest Transportation Center
U.S. DOT Office of the Assistant Secretary
for Research and Technology

MIDWEST
TRANSPORTATION
CENTER
MTC
IOWA STATE UNIVERSITY
Institute for Transportation

## About MTC

The Midwest Transportation Center (MTC) is a regional University Transportation Center (UTC) sponsored by the U.S. Department of Transportation Office of the Assistant Secretary for Research and Technology (USDOT/OST-R). The mission of the UTC program is to advance U.S. technology and expertise in the many disciplines comprising transportation through the mechanisms of education, research, and technology transfer at university-based centers of excellence. Iowa State University, through its Institute for Transportation (InTrans), is the MTC lead institution.

## About CTRE

The mission of the Center for Transportation Research and Education (CTRE) at Iowa State University is to develop and implement innovative methods, materials, and technologies for improving transportation efficiency, safety, and reliability while improving the learning environment of students, faculty, and staff in transportation-related fields.

## ISU Non-Discrimination Statement

Iowa State University does not discriminate on the basis of race, color, age, ethnicity, religion, national origin, pregnancy, sexual orientation, gender identity, genetic information, sex, marital status, disability, or status as a U.S. veteran. Inquiries regarding non-discrimination policies may be directed to Office of Equal Opportunity, 3410 Beardshear Hall, 515 Morrill Road, Ames, Iowa 50011, Tel. 515-294-7612, Hotline: 515-294-1222, email eooffice@iastate.edu.

## Notice

The contents of this report reflect the views of the authors, who are responsible for the facts and the accuracy of the information presented herein. The opinions, findings and conclusions expressed in this publication are those of the authors and not necessarily those of the sponsors.

This document is disseminated under the sponsorship of the U.S. DOT UTC program in the interest of information exchange. The U.S. Government assumes no liability for the use of the information contained in this document. This report does not constitute a standard, specification, or regulation.

The U.S. Government does not endorse products or manufacturers. If trademarks or manufacturers' names appear in this report, it is only because they are considered essential to the objective of the document.

## Quality Assurance Statement

The Federal Highway Administration (FHWA) provides high-quality information to serve Government, industry, and the public in a manner that promotes public understanding. Standards and policies are used to ensure and maximize the quality, objectivity, utility, and integrity of its information. The FHWA periodically reviews quality issues and adjusts its programs and processes to ensure continuous quality improvement.

## Iowa DOT Statements

Federal and state laws prohibit employment and/or public accommodation discrimination on the basis of age, color, creed, disability, gender identity, national origin, pregnancy, race, religion, sex, sexual orientation or veteran's status. If you believe you have been discriminated against, please contact the Iowa Civil Rights Commission at 800-457-4416 or the Iowa Department of Transportation affirmative action officer. If you need accommodations because of a disability to access the Iowa Department of Transportation's services, contact the agency's affirmative action officer at 800-262-0003.

## Technical Report Documentation Page

| 1. Report No. | 2. Government Accession No. | 3. Recipient's Catalog No. |
|---|---|---|
| IHRB Project TR-708D | | |

| 4. Title and Subtitle | 5. Report Date |
|---|---|
| Estimating Energy Efficiency of Connected and Autonomous Vehicles in a Mixed Fleet | May 2018 |
| | **6. Performing Organization Code** |

| 7. Author(s) | 8. Performing Organization Report No. |
|---|---|
| Jing Dong (orcid.org/0000-0002-7304-8430), Chaoru Lu (orcid.org/0000-0001-8418-7658), and Liang Hu (orcid.org/0000-0001-6351-8542) | |

| 9. Performing Organization Name and Address | 10. Work Unit No. (TRAIS) |
|---|---|
| Center for Transportation Research and Education<br>Iowa State University<br>2711 South Loop Drive, Suite 4700<br>Ames, IA 50010-8664 | **11. Contract or Grant No.**<br>Part of DTRT13-G-UTC37 |

| 12. Sponsoring Organization Name and Address | | 13. Type of Report and Period Covered |
|---|---|---|
| Midwest Transportation Center<br>2711 S. Loop Drive, Suite 4700<br>Ames, IA 50010-8664<br><br>Iowa Highway Research Board<br>Iowa Department of Transportation<br>800 Lincoln Way<br>Ames, IA 50010 | U.S. Department of Transportation<br>Office of the Assistant Secretary for Research and Technology<br>1200 New Jersey Avenue, SE<br>Washington, DC 20590 | Final Report<br>**14. Sponsoring Agency Code** |

**15. Supplementary Notes**

Visit www.intrans.iastate.edu for color pdfs of this and other research reports.


**16. Abstract**

Connected and autonomous vehicle (CAV) technologies are likely to be gradually implemented over time and in a traffic environment consisting of a significant share of alternative fuel vehicles, such as flexible-fuel, plug-in electric, and fuel cell vehicles. This work proposes the use of rule-based ecological adaptive cruise control strategies—the ecological smart driver model (Eco-SDM) for gasoline CAVs and the energy-efficient electric driving model ($E^3$DM) for electric CAVs (e-CAVs)—to improve the energy efficiency of individual vehicles and traffic flow.

By adjusting the spacing between the leading and the following vehicles, the Eco-SDM provides smoother deceleration and acceleration than the adaptive cruise control strategies based on intelligent driver model-adaptive cruise control (IDM-ACC) and the Nissan model (Nissan-ACC). The $E^3$DM is able to maintain high energy efficiency of regenerative braking by adjusting the spacing between the leading and the following vehicles.

To estimate vehicle energy consumption in a mixed traffic stream, the Virginia Polytechnic Institute and State University (Virginia Tech) microscopic energy and emission (VT-Micro) model was calibrated for gasoline vehicles and a power-based electricity consumption model that considers the impact of ambient temperature on auxiliary load was proposed for battery electric vehicles (BEVs). Single-lane vehicle dynamics in a traffic stream with a mix of CAVs and human-driven vehicles were simulated.

Results showed that the Eco-SDM and $E^3$DM outperform IDM-ACC and Nissan-ACC in terms of energy consumption. For Eco-SDM-based CAVs, the fuel saving benefit was greatest when a CAV is at the front of a platoon. For $E^3$DM-based e-CAVs, higher market penetration of e-CAVs may not result in higher energy efficiency of the entire fleet. Considering mixed traffic streams with BEVs and gasoline vehicles, the energy consumption of the entire fleet decreased when the market penetration of BEVs (which contains both e-CAVs and manual BEVs) increased. A higher ratio of e-CAVs to manual BEVs resulted in higher energy efficiency.


| 17. Key Words | 18. Distribution Statement |
|---|---|
| battery electric vehicles—connected and autonomous vehicles—ecological adaptive cruise control—energy consumption models—energy efficiency | No restrictions. |

| 19. Security Classification (of this report) | 20. Security Classification (of this page) | 21. No. of Pages | 22. Price |
|---|---|---|---|
| Unclassified. | Unclassified. | 48 | NA |

# ESTIMATING ENERGY EFFICIENCY OF CONNECTED AND AUTONOMOUS VEHICLES IN A MIXED FLEET

**Final Report**
**May 2018**

**Principal Investigator**
Jing Dong, Transportation Engineer
Center for Transportation Research and Education, Iowa State University

**Research Assistants**
Chaoru Lu and Liang Hu

**Authors**
Jing Dong, Chaoru Lu, and Liang Hu

Sponsored by
Midwest Transportation Center,
U.S. Department of Transportation
Office of the Assistant Secretary for Research and Technology,
and Iowa Highway Research Board
(IHRB Project TR-708D)

Preparation of this report was financed in part
through funds provided by the Iowa Department of Transportation
through its Research Management Agreement with the
Institute for Transportation

A report from
**Institute for Transportation**
**Iowa State University**
2711 South Loop Drive, Suite 4700
Ames, IA 50010-8664
Phone: 515-294-8103 / Fax: 515-294-0467
www.intrans.iastate.edu

## TABLE OF CONTENTS

## LIST OF FIGURES



## LIST OF TABLES

## ACKNOWLEDGMENTS

The authors would like to thank the Iowa Department of Transportation (DOT), Iowa Highway Research Board (IHRB), Midwest Transportation Center, and U.S. Department of Transportation Office of the Assistant Secretary for Research and Technology for sponsoring this project. This was one of four pilot projects for novel or innovative ideas and fundamental advances that were sponsored.

## EXECUTIVE SUMMARY

Connected and autonomous vehicle (CAV) technologies are likely to be gradually implemented over time. This project proposes the use of rule-based ecological adaptive cruise control (ACC) strategies—the ecological smart driver model (Eco-SDM) for gasoline CAVs and the energy-efficient electric driving model ($E^3$DM) for electric CAVs (e-CAVs)—to improve energy efficiency of individual vehicles and traffic flow.

By adjusting the spacing between leading and following vehicles, the Eco-SDM provides smoother deceleration and acceleration than the adaptive cruise control strategies based on the intelligent driver model (IDM-ACC) and the Nissan model (Nissan-ACC). The $E^3$DM is able to maintain high energy efficiency of regenerative braking by adjusting the spacing between leading and following vehicles.

To estimate vehicle energy consumption in a mixed fleet, the Virginia Polytechnic Institute and State University (Virginia Tech) microscopic energy and emission (VT-Micro) model is calibrated for gasoline vehicles, and a power-based electricity consumption model is developed for battery electric vehicles (BEVs). Single-lane vehicle dynamics in a traffic stream with a mix of CAVs and human-driven vehicles are simulated.

The key findings regarding the energy efficiency of gasoline CAVs in a traffic stream with mixed CAVs and human-driven vehicles were as follows:

- By simulating single-lane vehicle dynamics in a platoon with different percentages of CAVs, the result shows that CAVs are generally more fuel efficient than the manually driven vehicles.

- The Eco-SDM outperforms IDM-ACC and Nissan-ACC in terms of fuel efficiency and travel time.

- Higher market penetration of CAVs results in better fuel efficiency of the fleet. When the market penetration of Eco-SDM-equipped CAVs exceeds 30%, the marginal improvement of fuel efficiency decreases.

- One Eco-SDM CAV may result in up to 2% reduction in total fuel consumption if placed at the front of the platoon.

The key findings regarding the energy efficiency of electric CAVs in a traffic stream with mixed e-CAV and human-driven vehicles were as follows:

- By simulating single-lane vehicle dynamics in a platoon with different percentages of e-CAVs, the result shows that e-CAVs equipped with the $E^3$DM and Nissan-ACC consume less energy than the human-driven vehicles.

- The $E^3DM$ outperforms IDM-ACC, cooperative adaptive cruise control (CACC), and Nissan-ACC in terms of energy efficiency.

- Higher market penetration of e-CAVs may not result in better energy efficiency of the entire fleet. With the $E^3DM$, the highest energy efficiency is achieved when the market penetration of e-CAVs is 20%. This is because more e-CAVs in the traffic stream results in faster string stabilization and decreases the regenerative energy.

- Considering mixed traffic streams with BEVs (e-CAVs and manual-BEVs [m-BEVs]) and internal combustion engine vehicles (manual-ICEV), the marginal improvement in energy efficiency decreases when the market penetration of BEVs, including e-CAVs and m-BEVs, exceeds 20%.

- The larger the market penetration ratio of e-CAVs to m-BEVs is, the faster the marginal improvement in energy efficiency reaches the turning point.

## INTRODUCTION

In the United States, the fuel economy of personal vehicles is estimated as 24.7 miles per gallon (mpg) in 2016 and is projected to be 54.5 mpg in 2025 (EPA 2016). Previous studies have shown that driver behavior could affect the fuel economy of conventional gasoline vehicles by 10~40% (De Vlieger 1997, De Vlieger et al. 2000, Van Mierlo et al. 2004). Recent developments in advanced driving-assistance systems, such as adaptive cruise control (ACC), present opportunities to improve energy efficiency and fuel efficiency through automated vehicle operations. Several ACC methods have been proposed in the literature. For example, Davis (2004) proposed an ACC that automatically maintained a safe distance and minimized the speed difference between the following vehicle and its immediate preceding vehicle. Kesting et al. (2010) proposed an ACC based on the intelligent driver model (IDM) (which inherited its intuitive parameters from those proposed by Treiber et al. 2000) called IDM-ACC. A rule-based ACC, which is proprietary to Nissan, was described by Shladover et al. (2012), called Nissan-ACC. Furthermore, battery electric vehicle (BEV) technology is continuously implemented and considered as a solution to reduce oil dependence and vehicle emissions because of its high energy efficiency and zero tailpipe emissions (Jung and Jayakrishnan 2012, Yang et al. 2016). To further improve the driving efficiency and extend the vehicle range, an energy-efficient management strategy specifically for BEV is desired (Schwickart et al. 2015).

By modeling ACC-equipped vehicle behavior, the impact of ACC on traffic flow is widely studied (Fancher et al. 2002, Kikuchi et al. 2003, Liang and Peng 2000). Davis showed that ACC-equipped vehicles can suppress wide moving jams by making the flow string stable (Davis 2004). Kesting et al. (2008) reported that the traffic congestion was completely eliminated when the share of ACC-equipped vehicle reaches 25%. Moreover, by simulating a mixed traffic flow consisting of ACC-equipped and manually driven vehicles, Jiang et al. (2007) found that the introduction of ACC-equipped vehicles would enhance the free flow stability. Yuan et al. (2009) investigated the transition probability from synchronized flow to congestion and pointed out that ACC-equipped vehicles enhanced the traffic stability of the synchronized flow.

The energy efficiency of ACC-equipped vehicles has also been studied in the literature. Mersky and Samaras (2016) investigated the fuel efficiency of ACC based on existing fuel economy tests. The results showed that ACC-equipped vehicles can degrade fuel economy by up to 3%. To improve the energy efficiency of the vehicle system, one typical method is to optimize the vehicle speed profile with smoother deceleration and acceleration rates (Wu et al. 2015). Using simulations and experiments, Ioannou and Stefanovic (2005) found that the smooth response of ACC-equipped vehicles decreased the emissions even with the presence of disturbances that are due to high-acceleration maneuvers, lane cut-ins, and lane exiting. Several control strategies have been proposed to improve fuel efficiency or decrease emissions of ACC-equipped vehicles (Li et al. 2015a, Luo et al. 2015, Kamal et al. 2011). Park et al. (2012) and Ahn et al. (2013) developed eco-ACC systems based on optimal control and demonstrated its potential in improving fuel efficiency. Yang et al. (2017) developed an eco-cooperative ACC, which computes the fuel-optimum vehicle trajectory through a signalized intersection. Vajedi and Azad (2016) proposed an eco-ACC for the Toyota Prius Plug-in Hybrid to reduce the total energy cost. Moreover, considering ACC-equipped vehicles in a mixed traffic environment, Wang et al. (2015) proposed two model predictive control (MPC)-based control strategies. The simulation

results showed that a 20% share of ACC-equipped vehicles could reduce emissions of a platoon of vehicles by 18~27%. Moreover, Li et al. (2015b) studied the performance of a fuel-optimized ACC strategy, called pulse-and-glide, on traffic smoothness and fuel economy in a mixed traffic flow. They pointed out that a pulse-and-glide strategy can significantly decrease the fuel consumption of individual vehicles. However, the fuel consumption of the platoon, which contains ACC-equipped and manually driven vehicles, may increase with an under-damped pattern. In summary, most of the existing ecological ACC strategies are formulated as an optimization problem. For this work, a rule-based ecological ACC system is proposed and tested using a fuel consumption model that is calibrated using on-road fuel economy data.

Recently, a few ACC models have been proposed for electric vehicles (Huang and Wang 2012, Wu et al. 2015, Zhang et al. 2017). For regenerative braking control, Huang and Wang (2012) proposed a nonlinear model predictive controller that is capable of restoring more regenerative braking energy than a conventional controller. Based on forward terrain profile preview information, Chen and Wang (2014) and Chen et al. (2014) introduced an energy-efficient driving control strategy that can optimally distribute the torque between the front and rear motors to save driving energy.

Akhegaonkar et al. (2016) proposed a longitudinal controller to minimize energy consumption and maximize energy regeneration. Schwickart et al. (2016) designed an ACC system based on a model predictive control method with a quadratic cost function, a linear prediction model, and linear constraints. Considering terrain characteristics and preceding vehicle information, Zhang et al. (2017) developed an energy management strategy for BEVs equipped with in-wheel motors. The simulation results showed that using the preceding vehicle movement information results in additional energy savings.

In summary, most of the existing energy-efficient ACC strategies are formulated as optimization problems, using either global or local optimization methods, such as particle swarm optimization and model predictive control. In particular, the existing control strategies for BEVs mostly focused on optimizing the speed profile of individual vehicles. The main drawbacks of optimization-based approaches are the complicity and computational intensity. Rule-based control strategies, on the other hand, have monopolized the production vehicle market because of their low computational demand, natural adaptability to online applications, and reliability (Enang and Bannister 2017).

Furthermore, connected and autonomous vehicle (CAV) technologies are likely to be gradually implemented over time. Thus, CAV and manually driven vehicles are likely to share the road network in the near future. The environmental benefit may vary with the location and penetration of CAVs in the string of mixed traffic (Ioannou and Stefanovic 2005). In addition, in a mixed traffic stream, the fuel-saving of individual vehicles does not always result in fuel-saving of the entire system. Therefore, the location of CAVs in a platoon need to be taken into account when designing ACC systems that are targeted at decreasing the energy consumption of individual vehicles and the entire system.

In this project, two rule-based energy-efficient ACC models are proposed, considering a mixed traffic stream with CAVs and human-driven vehicles. The proposed ACC systems are evaluated using the energy consumption models developed and calibrated based on on-road vehicle fuel economy data. The impacts of ACC strategies on energy consumption were investigated using an urban driving cycle.

This report is organized as follows. First, car-following models for human drivers, adaptive cruise control, and cooperative adaptive cruise control are reviewed. Two adaptive cruise control models are proposed for gasoline CAVs and electric CAVs, respectively. Then, the Virginia Polytechnic Institute and State University (Virginia Tech) microscopic energy and emission (VT-Micro) fuel consumption model is calibrated for gasoline vehicles and a BEV electricity consumption model is proposed. These models were used to estimate vehicle energy consumption in the simulation study. After that, the energy efficiency of gasoline CAVs and electric CAVs in a mixed fleet are evaluated. Finally, the conclusions and key findings are summarized.

## SIMULATION OF MANUAL VEHICLES AND CAVS USING CAR-FOLLOWING MODELS

### Review of Existing Car-Following Models

*Human Driver Car-following Models*

In the past decades, a number of car-following models have been introduced to simulate human driver behavior (Newell 1961, Talebpour et al. 2011). In particular, based on the Gipps model (Gipps 1981), Treiber et al. (2000) proposed a human driver model named the intelligent driver model (IDM). Since the IDM provides greater realism than most of the deterministic acceleration modeling frameworks, it is widely applied to investigate the impact of autonomous vehicles on traffic flow stability, fuel consumption, and emissions in traffic streams with mixed autonomous and human-driven vehicles (Li et al. 2015b, Talebpour and Mahmassani 2016, Wang et al. 2015). Accordingly, the IDM was used in this study to simulate the human-driven vehicles. The IDM is formulated as follows:

$$a_{IDM}^{n} = a_{max}\left[1 - \left(\frac{v_n}{v_0}\right)^{\delta} - \left(\frac{s^*}{\Delta x}\right)^2\right] \quad (1)$$

$$s^* = s_0 + v_n T + \frac{v_n(v_n - v_{n-1})}{2\sqrt{a_{max} b}} \quad (2)$$

where
$a_{IDM}^{n}$ is the acceleration of the following vehicle (m/s$^2$)
$\delta$ is the acceleration exponent
$s_0$ is the standstill distance between stopped vehicles (m)
$a_{max}$ is the maximum acceleration (m/s$^2$)
$\Delta x$ is the spacing between the leading and the following vehicle (m)
$T$ is the desired time headway (s)
$v_0$ is the maximum speed (m/s)
$v_n$ is the speed of the following vehicle (m/s)
$v_{n-1}$ is the speed of the leading vehicle (m/s)
$s^*$ is the desired spacing (m)
$b$ is the desired deceleration (m/s$^2$)

*Adaptive Cruise Control*

In recent years, car-following models have evolved to describe the behavior of vehicles with advanced cruise controls, which take advantage of the sensing and communication technologies. Several rule-based ACC models have been proposed in the literature (e.g., Davis 2004, Kesting et al. 2010, and Shladover et al. 2012). In particular, Kesting et al. (2010) proposed an ACC based on the IDM, called IDM-ACC, which inherited the parameters proposed by Treiber et al.

(2000). The acceleration according to the constant-acceleration heuristic (CAH) is written as follows:

$$a_{CAH}^{n} = \begin{cases} \frac{v_n^2 \tilde{a}_l}{v_{n-1}^2 - 2\Delta x \tilde{a}_l} & if\ v_n(v_n - v_{n-1}) \leq -2\Delta x \tilde{a}_l \\ \tilde{a}_l - \frac{(v_n - v_{n-1})^2 \Theta(v_n - v_{n-1})}{2\Delta x} & otherwise \end{cases} \quad (3)$$

where
$a_{CAH}^{n}$ is the constant-acceleration heuristic acceleration of the following vehicle (m/s$^2$)
$\Theta$ is the Heaviside step function
$a_{n-1}$ is the acceleration of the leading vehicle
$\tilde{a}_l$ is the effective acceleration used to avoid artefacts that may be caused by leading vehicles with higher acceleration capabilities, and $\tilde{a}_l = \min(a_{n-1}, a_{max})$

The adaptive cruise control based on the IDM is formulated as follows:

$$a_{IDM-ACC}^{n} = \begin{cases} a_{IDM}^{n} & a_{IDM}^{n} \geq a_{CAH}^{n} \\ (1-c)a_{IDM}^{n} + c\left[a_{CAH}^{n} + b\tanh\left(\frac{a_{IDM}^{n} - a_{CAH}^{n}}{b}\right)\right] & otherwise \end{cases} \quad (4)$$

where
$a_{IDM-ACC}^{n}$ is the acceleration of the following vehicle equipped with IDM-ACC (m/s$^2$)
$c$ is the coolness factor

Another rule-based ACC strategy, which is proprietary to Nissan and was described by Shladover et al. (2012), is called the Nissan-ACC model. The simplified representations of the Nissan-ACC model contain speed control and spacing control. In the speed control, the control law is as follows:

$$v_e = v_n - v_0 \quad (5)$$

$$a_{sc} = bound(-0.4 \times v_e, a_{max}, b_{max}) \quad (6)$$

$$a_{Nissan-ACC}^{n} = a_{sc} \quad (7)$$

where
$a_{Nissan-ACC}^{n}$ is the acceleration of the following vehicle equipped with Nissan-ACC (m/s$^2$)
$b_{max}$ is the maximum deceleration (m/s$^2$)
$a_{sc}$ is the acceleration by speed control (m/s$^2$)
$v_e$ is the speed error (m/s)

The function bound ( ) is defined as bound ($x$, $x_{ub}$, $x_{lb}$) = max(min($x$, $x_{ub}$), $x_{lb}$), where $x_{ub}$ is the upper bound and $x_{lb}$ is the lower bound. This function restricts the acceleration to the range between the maximum acceleration and deceleration.

In the spacing control, the speed control law also applies. In addition, to maintain a constant time headway between vehicles, the spacing control law requires the following:

$$s^* = T \times v_n \tag{8}$$

$$s_e = \Delta x - s^* \tag{9}$$

$$a^n_{Nissan-ACC} = bound(\dot{s} + 0.25 \times s_e, a_{sc}, b_{max}) \tag{10}$$

where
$\dot{s}$ is the acceleration adjustment parameter (m/s$^2$)

When $v_{n-1} = 0$, $v_n = 0$ and $s_e = s_0$, $a^n_{Nissan\_ACC}$ should equal 0. Since the desired speed and maximum acceleration are larger than 0, we have the following:

$$a_{sc} = bound(0.4 \times v_0, a_{max}, b_{max}) > 0 \tag{11}$$

Since $a^n_{Nissan\_ACC} = 0$ and $a_{sc} > 0$, $\dot{s} + 0.25 \times s_0$ should equal 0. Therefore, the acceleration adjustment parameter ($\dot{s}$) can be derived as follows:

$$\dot{s} = -0.25 \times s_0 \tag{12}$$

As a result, the spacing control law is modified as follows:

$$s^* = T \times v_n + s_0 \tag{13}$$

$$s_e = \Delta x - s^* \tag{14}$$

$$a^n_{Nissan-ACC} = bound(0.25 \times s_e, a_{sc}, b_{max}) \tag{15}$$

*Cooperative Adaptive Cruise Control*

As an extension of ACC, several cooperative ACC (CACC) strategies have been proposed, e.g., Shladover et al. (2012), Dey et al. (2016), Milanés and Shladover (2014), and Xiao et al. (2017). In particular, Van Arem et al. (2006) proposed a CACC in which the acceleration at every decision point is calculated as follows:

$$a_{CACC}^{n} = min(\, a_d, k(v_0 - v_n)) \tag{16}$$

$$a_d = k_a a_{n-1} + k_v(v_{n-1} - v_n) + k_d(\Delta x - s^*) \tag{17}$$

$$s^* = max\left(Tv_n, s_0, \frac{v_n^2}{2}\left(\frac{1}{d_p} - \frac{1}{d}\right)\right) \tag{18}$$

where
$k_a$, $k_v$, and $k_d$ are constants
$d_p$ and $d$ are the deceleration capabilities of the leading and following vehicles, which are equal to $b_{max}$ in this report
$k$ is the constant-speed error factor

Based on the recommendations of Van Arem et al. (2006), $= 1$, $k_a = 1$, $k_v = 0.58$, and $k_d = 0.1$.

In this study, IDM-ACC, Nissan-ACC, and Van Arem CACC are applied to simulate the CAVs. The performance of these models are compared with the proposed energy-efficient ACC model.

**Adaptive Cruise Control for CAVs**

A single-lane car-following scenario is considered to derive the properties of the proposed ACCs. The following assumptions are made: (1) only CAVs are capable of communicating with other CAVs through vehicle-to-vehicle communication, which is an ideal wireless connection (Davis 2017); (2) on-board sensors measure vehicle speed, gap (relative distance), and relative speed with respect to the preceding vehicle at regular time intervals (Wang et al. 2018); and (3) there is no computational, sensor, or communication delays for CAVs.

An example of a platoon containing CAVs and manually driven vehicles is shown in Figure 1.

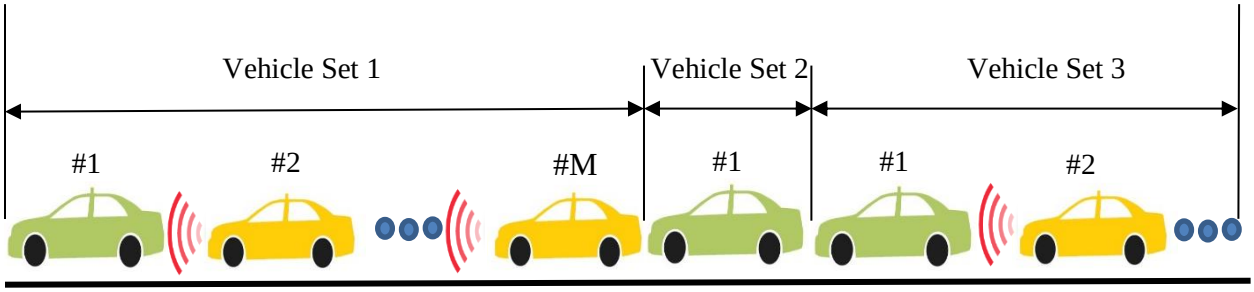


**Figure 1. A platoon with CAVs (yellow) and manually driven vehicles (green)**

The manually driven vehicles and CAVs are represented by green vehicles and yellow vehicles, respectively. According to the aforementioned assumptions, only CAVs can share the information and the CAV can detect the manually driven vehicle immediately in front of it.

Therefore, the number of manually driven vehicles between CAVs is unknown. As a result, manually driven vehicles separate the platoon into several vehicle sets. A manually driven vehicle is always the first vehicle in a vehicle set. That is, the location (*N*) of a manually driven vehicle is labeled as 1. The locations of CAVs in the vehicle sets are labeled as 2 to *M*. Note that the vehicle set definition is used to determine the location of CAVs and design the ACC strategies. A manually driven vehicle can still follow a CAV in the platoon, according to its car-following rules.

*Ecological Smart Driver Model for Gasoline CAVs*

Most of the existing ecological cruise control methods are optimization-based and do not consider the location of CAVs in a platoon. A rule-based ecological ACC model, named the ecological smart driver model (Eco-SDM) is proposed (Lu et al. 2018). The acceleration of a following vehicle equipped with the Eco-SDM is determined by the following equation:

$$a_{Eco-SDM}^{n} = a_{max} - \frac{a_{max}+\frac{v_n^2-v_{n-1}^2}{2\Delta x}}{e^{\left(\frac{\Delta x}{s_0+v_n\times T}-1-\beta\times\frac{v_n}{v_0}\times\frac{(v_0-v_n)}{v_0}\right)}} \tag{19}$$

where,
$a_{Eco-SDM}^{n}$ is the acceleration of the following vehicle that is equipped with the Eco-SDM (m/s$^2$)
$\beta$ is an adjust parameter considering the location of the CAV in the vehicle set

In addition, the maximum speed constraint requires $v \leq v_0$, which guarantees a speed not exceeding the maximum speed.

To stabilize the string of vehicles in a mixed traffic stream quickly, the CAVs located closer to the manually driven vehicles need to react more dramatically to attenuate the disturbance from manually driven vehicles in front of them. Therefore, the parameter ($\beta$) of the Eco-SDM is determined as follows:

$$\beta = \frac{1}{ln(N)} + 1 \tag{20}$$

where,
$N$ is the location of a CAV in a vehicle set, and $N \geq 2$

According to Equation 19 and Equation 20, CAVs with the Eco-SDM tend to accelerate with $a_{max}$ when $\Delta x$ is large. A CAV will brake when the speed of the CAV is greater than the leading vehicle speed and $\Delta x$ is less than the desired spacing. When there is no speed difference between the leading and following vehicles, a CAV's acceleration increases with the ratio of $\Delta x$ to the desired spacing. According to the characteristics of the exponential function, the jerk of the CAV, which represents the changing rate of a CAV's acceleration, decreases with the ratio of $\Delta x$ to the desired spacing. Moreover, a CAV would adjust its speed-dependent spacing based on the

location of the CAV in a vehicle set. Consequently, the CAVs equipped with the Eco-SDM can achieve smoother acceleration and deceleration.

Several properties of the Eco-SDM are discussed as follows, considering special cases.

First, when a CAV is cruising (i.e., $a^n_{Eco-SDM} = 0$ and $v_n - v_{n-1} = 0$), the speed-dependent spacing $\Delta x$ between the preceding and the following vehicles are given by the following:

$$\Delta x = \left(1 + \beta \times \frac{v_n}{v_0} \times \frac{(v_0 - v_n)}{v_0}\right)(s_0 + v_n \times T) \tag{21}$$

In particular, when the vehicle is stopped or reached the maximum speed (i.e., $v_n = 0$ or $v_n = v_0$), the speed-dependent spacing $\Delta x$ equals the desired spacing, which is $\Delta x = s_0 + v_n \times T$. The desired spacing is composed of a standstill distance ($s_0$) and a speed-dependent term, $v_n T$. When a CAV follows other CAVs, β decreases with the location (*N*), and the speed-dependent spacing $\Delta x$ of the CAV is closer to the desired spacing. Note that in equilibrium traffic of arbitrary density, the speed-dependent spacing $\Delta x$ of both the IDM-ACC and Nissan-ACC models are the desired spacing, while the speed-dependent spacing $\Delta x$ of the Eco-SDM would only equal the desired spacing when $v_n$ is equal to 0 or $v_0$.

Second, when the traffic density is low (i.e., $\Delta x$ is large), CAVs will accelerate to the maximum speed. When $\Delta x \to \infty$, $\frac{v_n^2 - v_{n-1}^2}{2\Delta x}$ is close to 0. At the same time, $e^{\left(\frac{\Delta x}{s_0 + v_n \times T} - 1 - \beta \times \frac{v_n}{v_0} \times \frac{(v_0 - v_n)}{v_0}\right)}$ is close to infinity. As a result, the acceleration with the Eco-SDM is approximately equal to the maximum acceleration, i.e., $a^n_{Eco-SDM} \approx a$. After the speed of the CAV reaches the maximum speed, acceleration with the Eco-SDM is 0.

Third, when a CAV is following a slower vehicle or approaching a stopped vehicle (i.e., $v_n - v_{n-1} > 0$) with the limited spacing ($\Delta x \to s_0 + v_0 \times T$), the acceleration equation of the Eco-SDM is given by the following:

$$a^n_{Eco-SDM} \to a_{max} - \frac{a_{max} + \frac{v_n^2 - v_{n-1}^2}{2(s_0 + v_n \times T)}}{exp\left(-\beta \times \frac{v_n}{v_0} \times \frac{(v_0 - v_n)}{v_0}\right)} \tag{22}$$

Specifically, when a CAV with the maximum speed approaches a stopped vehicle (i.e., $v_n = v_0$, $v_{n-1} = 0$), the maximum kinematic deceleration is applied to avoid a collision, as follows:

$$a^n_{Eco-SDM} = -\frac{V_0^2}{2(s_0 + v_0 \times T)} \tag{23}$$

Fourth, when the spacing is much less than the desired spacing ($\Delta x \ll s_0 + v_0 \times T$) and there are no significant speed differences ($v_n - v_{n-1} \approx 0$), the acceleration is determined as follows:

$$a_{Eco-SDM}^{n} \approx a_{max}\left(1-\frac{1}{e^{\left(\frac{\Delta x}{s_0+v_n\times T}-1-\beta\times\frac{v_n}{v_0}\times\frac{(v_0-v_n)}{v_0}\right)}}\right) \quad (24)$$

Specifically, when $\Delta x \to 0$, Equation 24 reduces to the following:

$$a_{Eco-SDM}^{n} \approx a_{max}\left(1-\frac{1}{e^{\left(-1-\beta\times\frac{v_n}{v_0}\times\frac{(v_0-v_n)}{v_0}\right)}}\right) \quad (25)$$

Since $\beta\times\frac{v_n}{v_0}\times\frac{(v_0-v_n)}{v_0}$ is always greater than 0, $e^{\left(-1-\beta\times\frac{v_n}{v_0}\times\frac{(v_0-v_n)}{v_0}\right)}$ is always less than 1. The following vehicle will adjust its deceleration according to its speed.

*Energy-Efficient Electric Driving Model ($E^3DM$) for E-CAVs*

Existing energy-efficient BEV cruise control strategies are optimization-based and do not consider mixed traffic consisting of autonomous and human-driven vehicles. A rule-based ACC, named the energy-efficient electric driving model ($E^3DM$), is proposed for BEVs in mixed traffic streams. Fiori et al. (2016) showed that a marginal increment of energy regeneration efficiency decreases exponentially with the increase of deceleration. Thus, to achieve high energy efficiency of regenerative braking, the electric-CAVs (e-CAVs) should maintain a small deceleration for a long duration instead of applying a large deceleration for a short duration. Consequently, the acceleration of a following vehicle equipped with the $E^3DM$ is determined by the following equation:

$$a_{E^3DM}^{n} = a_{max}\times\left[1-\left(\frac{v_n}{v_0}\right)^4\right]-\frac{a_{max}\times\left[1-\left(\frac{v_n}{v_0}\right)^4\right]+\frac{v_n^2-v_{n-1}^2}{2\Delta x}}{e^{\frac{\Delta x}{s_0+v_n\times T+\frac{v_n(v_n-v_{n-1})}{2\beta\sqrt{a_{max}b}}}-1-\beta^2\times\frac{v_n}{v_0}\times\left[\frac{(v_0-v_n)}{v_0}\right]^{\gamma}}} \quad (26)$$

where
$a_{E^3DM}^{n}$ is the acceleration of the following vehicle that is equipped with the $E^3DM$ ($m/s^2$)
$\gamma$ is a parameter indicating the preceding vehicle type

The parameter ($\gamma$) of the $E^3DM$ is determined as follows:

$$\gamma=\begin{cases}1, & if\ follows\ an\ \text{e–CAV}\\ 0.5, & else\end{cases} \quad (27)$$

According to Equation 26 and Equation 27, e-CAVs with the $E^3DM$ accelerate with $a_{max}\left[1-\left(\frac{v_n}{v_0}\right)^4\right]$ when $\Delta x$ is large, which is the same as with the IDM (Treiber et al. 2000). An e-CAV will brake while the speed of the e-CAV is greater than the leading vehicle speed and $\Delta x$

is less than the desired spacing. When there is no speed difference between the leading and following vehicle, an e-CAV's acceleration increases with the ratio of $\Delta x$ to the desired spacing.

According to the characteristics of the exponential function, the jerk of an e-CAV, which represents the changing rate of an e-CAV's acceleration, decreases with the ratio of Δx to the desired spacing. Moreover, an e-CAV adjusts its speed-dependent spacing based on the location of the e-CAV in a vehicle set and type of leading vehicle. Consequently, the e-CAVs equipped with the E$^3$DM can achieve smooth acceleration and efficient regenerative braking.

Several properties of the E$^3$DM are discussed as follows, considering special cases.

First, when an e-CAV is cruising (i.e., $a^n_{E^3DM} = 0$ and $v_n - v_{n-1} = 0$), the speed-dependent spacing $\Delta x$ between the preceding and the following vehicle is given by the following:

$$\Delta x = \left(1 + \beta^2 \times \frac{v_n}{v_0} \times \left[\frac{(v_0 - v_n)}{v_0}\right]^\gamma\right)(s_0 + v_n \times T) \tag{28}$$

In particular, when the vehicle is stopped or reached the maximum speed (i.e., $v_n = 0$ or $v_n = v_0$), speed-dependent spacing $\Delta x$ equals the desired spacing, that is, $\Delta x = s_0 + v_n \times T$. The desired spacing is composed of a standstill distance ($s_0$) and an additional speed-dependent term, $v_n T$. When an e-CAV follows other e-CAVs, β decreases with the location (*N*), and the speed-dependent spacing $\Delta x$ of the e-CAV is closer to the desired spacing. Note that in equilibrium traffic of arbitrary density, the speed-dependent spacing $\Delta x$ of both the IDM-ACC and Nissan-ACC models are the desired spacing, while the speed-dependent spacing $\Delta x$ of the E$^3$DM would only equal the desired spacing when $v_n$ is equal to 0 or the maximum speed.

Second, when the traffic density is low (i.e., $\Delta x$ is large), e-CAVs will accelerate to the maximum speed. When $\Delta x \to \infty$, $\frac{v_n^2 - v_{n-1}^2}{2\Delta x}$ is close to 0. At the same time $e^{\left(\frac{\Delta x}{s_0 + v_n \times T + \frac{v_n(v_n - v_{n-1})}{2\beta\sqrt{ab}}} - 1 - \beta^2 \times \frac{v_n}{v_0} \times \left[\frac{(v_0 - v_n)}{v_0}\right]^\gamma\right)}$ is close to infinity. As a result, the acceleration of the E$^3$DM is approximately equal to the maximum acceleration, $a^n_{E^3DM} \approx a$. After the speed reaches the maximum speed, acceleration of the E$^3$DM is 0.

Third, when an e-CAV is following a slower vehicle or approaching a stopped vehicle (i.e., $v_n - v_{n-1} > 0$) with a limited spacing ($\Delta x \to s_0 + v_0 \times T$), the acceleration equation is given by

$$a^n_{E^3DM} \to a_{max} \times \left[1 - \left(\frac{v_n}{v_0}\right)^4\right] - \frac{a_{max} \times \left[1 - \left(\frac{v_n}{v_0}\right)^4\right] + \frac{v_n^2 - v_{n-1}^2}{2(s_0 + v_n \times T)}}{exp\left(-\beta^2 \times \frac{v_n}{v_0} \times \left[\frac{(v_0 - v_n)}{v_0}\right]^\gamma\right)} \tag{29}$$

Specifically, when an e-CAV with the maximum speed approaches a stopped vehicle (i.e., $v_n = v_0, v_{n-1} = 0$), the maximum kinematic deceleration is applied to avoid a collision, as follows:

$$a_{E^3DM}^n = -\frac{V_0^2}{2(s_0+v_0\times T)} \tag{30}$$

Fourth, when the spacing is much smaller than the desired spacing ($\Delta x \ll s_0 + v_0 \times T$) and there are no significant speed differences ($v_n - v_{n-1} \approx 0$), the acceleration is determined as follows:

$$a_{E^3DM}^n \approx a_{max} \times \left[1 - \left(\frac{v_n}{v_0}\right)^4\right] - \frac{a_{max}\times\left[1-\left(\frac{v_n}{v_0}\right)^4\right]}{e^{\frac{\Delta x}{s_0+v_n\times T+\frac{v_n(v_n-v_{n-1})}{2\beta\sqrt{ab}}}-1-\beta^2\times\frac{v_n}{v_0}\times\left[\frac{(v_0-v_n)}{v_0}\right]^\gamma}} \tag{31}$$

Specifically, when $\Delta x \to 0$, Equation 31 reduces to

$$a_{E^3DM}^n \approx a_{max} \times \left[1 - \left(\frac{v_n}{v_0}\right)^4\right] \times \left(1 - \frac{1}{e^{-1-\beta^2\times\frac{v_n}{v_0}\times\left[\frac{(v_0-v_n)}{v_0}\right]^\gamma}}\right) \tag{32}$$

Since $\beta^2 \times \frac{v_n}{v_0} \times \left[\frac{(v_0-v_n)}{v_0}\right]^\gamma$ is always greater than 0, $e^{-1-\beta^2\times\frac{v_n}{v_0}\times\left[\frac{(v_0-v_n)}{v_0}\right]^\gamma}$ is always less than 1. The following vehicle will adjust its deceleration according to its speed.

In the numerical experiment, a traffic stream containing both CAVs and human-driven vehicles is simulated. The IDM is used to describe the driver behavior of the human-driven vehicles. The CAVs are simulated using the Eco-SDM, IDM-ACC, and Nissan-ACC models. Meanwhile, the e-CAVs are simulated using the E$^3$DM, IDM-ACC, Nissan-ACC, and CACC models. The acceleration model parameters of the human-driven vehicles and CAVs are based on the parameters of IDM proposed by Kesting et al. (2010), as listed in Table 1.

**Table 1. Parameters of the acceleration models**

| Parameters | IDM | IDM-ACC | Nissan-ACC | E$^3$DM | Eco-SDM | CACC |
|---|---|---|---|---|---|---|
| Maximum speed $v_0$ (m/s) | | | | | 33.3 | |
| Free acceleration exponent $\delta$ | 4 | 4 | — | — | — | — |
| Desired time headway $T$ (s) | | | | | 1.5 | |
| Standstill distance $s_0$ (m) | | | | | 2 | |
| Maximum acceleration $a_{max}$ (m/s$^2$) | | | | | 1.4 | |
| Desired deceleration $b$ (m/s$^2$) | 2 | 2 | — | 2 | — | — |
| Maximum deceleration $b_{max}$ (m/s$^2$) | | | | | 6 | |
| Coolness factor $c$ | — | 0.99 | — | — | — | — |

## ESTIMATED ENERGY CONSUMPTION OF GASOLINE VEHICLES AND BEVS

### Fuel Consumption Model for Gasoline Vehicles

*Review of Fuel Consumption Models*

Various fuel consumption models of gasoline vehicles have been proposed in the literature. Since vehicle speed and acceleration data can be collected by various devices, such as on-board diagnostics (OBD-II) loggers, on-board trackers and smartphones, instantaneous speed and acceleration are widely used as predictors to estimate vehicle fuel consumption. One pioneer work was done by Ahn et al. (2002) and Rakha and Ahn (2004) who proposed the Virginia Tech microscopic energy and emission (VT-Micro) model. This regression model takes polynomial combinations of speed and acceleration levels as the explanatory variables to estimate vehicle fuel consumption. Kamal et al. (2011) also developed a regression-based fuel consumption model that is similar to VT-Micro, but took different polynomial terms of speed and acceleration into account. Road inclination, if collected simultaneously with speed and acceleration, can also be included as an extra variable in fuel consumption estimation, such as by Ribeiro et al. (2013).

In addition to the above-mentioned regression models, some power-based models have been proposed as well. These models first calculated the instantaneous power of engines based on vehicle speed and acceleration, and then established the relationships between fuel consumption and engine power. For example, the Virginia Tech comprehensive power-based fuel consumption model (VT-CPFM) (Park et al. 2013, Rakha et al. 2011) estimated vehicle fuel consumption using the linear and quadratic terms of engine power. The model avoids bang-bang control and can be calibrated using publicly available data.

*Calibration and Validation of the VT-Micro Model*

This study adopts the VT-Micro model developed by Ahn et al. (2002) to estimate fuel consumption of gasoline vehicles. VT-Micro is a hybrid linear regression model, which includes a combination of linear, quadratic, and cubic speed and acceleration terms. The model has two parts based on the value of acceleration, as shown by Equation 33 and Equation 34.

$$\ln FC = \sum_{i=0}^{3}\sum_{j=0}^{3} L_{i,j} v^i a^j \quad (a \geq 0) \tag{33}$$

$$\ln FC = \sum_{i=0}^{3}\sum_{j=0}^{3} M_{i,j} v^i a^j \quad (a < 0) \tag{34}$$

where
$FC$ is fuel consumption rate (mL/s)
$v$ is vehicle speed (m/s)
$a$ is vehicle acceleration (m/s$^2$)
$L_{i,j}$ are regression parameters for $a \geq 0$
$M_{i,j}$ are regression parameters for $a < 0$

The data used to calibrate model parameters were collected using an OBD-II logger and a Global Positioning System (GPS) device installed on a passenger vehicle (2010 Honda CR-V) for seven months from October 2016 to May 2017. This vehicle was primarily used for daily commute between home and work, and was driven mainly on urban roads and major highways. A total of 543 trips were recorded. The OBD-II logger collected instantaneous fuel consumption every five seconds. The GPS device collected vehicle speed every one second. The acceleration is calculated based on the difference in vehicle speeds. By fitting linear regression models between instantaneous fuel consumptions, speeds, and accelerations, the regression coefficients specific to the vehicle are determined. The adjusted R-squared is 0.8245 when $a \geq 0$, and 0.6616 when $a < 0$. In addition, the chi-squared goodness-of-fit test is conducted based on the actual and the estimated instantaneous fuel consumptions. The p-value is 0.2416 when $a \geq 0$ and 0.2685 when $a < 0$, indicating the estimated instantaneous fuel consumption is not significantly different from the actual one. The regression coefficients are listed in Table 2 and Table 3.

**Table 2. Parameters of the calibrated VT-Micro model for $a \geq 0$**

| $a \geq 0$ | Constant | $v$ | $v^2$ | $v^3$ |
|---|---|---|---|---|
| **Constant** | -1.23E+00 | 6.05E-02 | 3.62E-04 | -2.22E-06 |
| $a$ | 4.69E-01 | 3.39E-01 | -1.91E-02 | 2.56E-04 |
| $a^2$ | -4.54E-02 | -1.33E-01 | 7.45E-03 | -5.44E-05 |
| $a^3$ | 1.34E-02 | 2.08E-02 | -2.01E-03 | 3.19E-05 |

**Table 3. Parameters of the calibrated VT-Micro model for $a < 0$**

| $a < 0$ | Constant | $v$ | $v^2$ | $v^3$ |
|---|---|---|---|---|
| **Constant** | -7.89E-01 | -2.14E-02 | 5.61E-03 | -9.16E-05 |
| $a$ | 2.83E-01 | -1.02E-01 | 2.01E-02 | -4.43E-04 |
| $a^2$ | 1.39E-01 | -7.45E-02 | 1.40E-02 | -3.44E-04 |
| $a^3$ | 9.13E-03 | -9.58E-03 | 2.16E-03 | -5.77E-05 |

The accuracy of the calibrated VT-Micro model is evaluated on a trip basis. The actual and estimated trip-level fuel consumptions are compared, as shown in Figure 2.

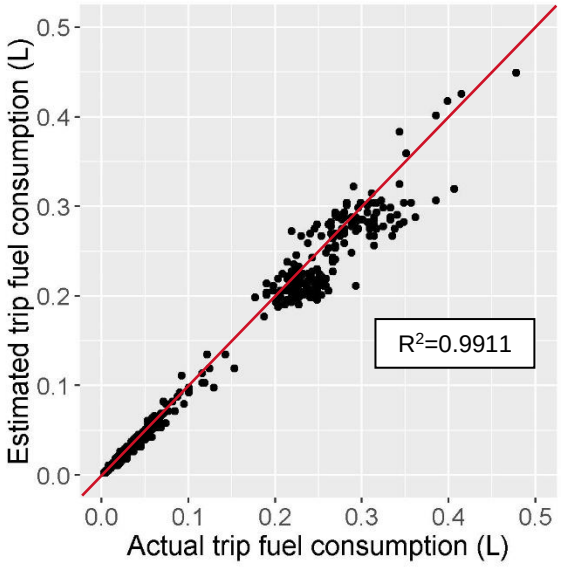


**Figure 2. Validation of the calibrated VT-Micro model**

The dots are mostly distributed along the diagonal line. The mean absolute percentage error (MAPE) and the root mean square error (RMSE) are computed as follows:

$$MAPE = \frac{1}{n}\sum_{i=1}^{n}\left|\frac{FC_{a,i}-FC_{e,i}}{FC_{a,i}}\right| \times 100\% \quad (35)$$

$$RMSE = \sqrt{\frac{\sum_{i=1}^{n}(FC_{a,i}-FC_{e,i})^2}{n}} \quad (36)$$

where
$FC_{e,i}$ is the estimated fuel consumption of trip $i$ (L)
$FC_{a,i}$ is the actual fuel consumption of trip $i$ (L)
$n$ is the total number of trips in the dataset ($n = 543$)

Both metrics have low values: MAPE equals 9.76% and RMSE equals 0.069 L. Therefore, the calibrated VT-Micro model is adequate for estimating vehicle fuel consumption at the trip level and is applied in the subsequent simulation.

## Energy Consumption Model for BEVs

### *Review of BEV Energy Consumption Models*

To assess energy efficiency of electric vehicles in a mixed traffic stream, appropriate energy consumption models are needed. Using the controller area network (CAN) bus and GPS trajectory data, several BEV energy consumption models have been proposed in the literature. Yao et al. (2014) used instantaneous speeds and accelerations as predictors to estimate BEV

energy consumption rate. In their subsequent work, battery state of charge (SOC) was also taken into account as the energy consumption rate was found to be negatively correlated with SOC (Zhang and Yao 2015). Liu et al. (2017(b)) studied the effects of road gradients on electricity consumption and found that the consumption increases almost linearly with the absolute gradient increases. Wang et al. (2017) studied the impact of ambient temperature on BEV energy usage and used a third-order polynomial regression model to describe the relationship between energy efficiency and temperature. Another commonly used predictor in energy consumption models is vehicle specific power (VSP) that can be gauged by vehicle speed and acceleration. For example, Alves et al. (2016) and Yao et al. (2014) developed hybrid regression models to estimate BEV energy consumption based on different levels of VSP. One important feature of BEVs is regenerative braking—when the vehicle decelerates, the electric motor converts kinetic energy to electricity that can be stored in batteries. Researchers have not reached consensus on the energy efficiency of regenerative braking as it is a complex process. Fiori et al. (2016) modeled regenerative energy as a function of deceleration levels in their BEV energy consumption model, while Yang et al. (2014) and Genikomsakis and Mitrentsis (2017) assumed that regenerative braking efficiency is linearly related to vehicle speed.

This section introduces two BEV energy consumption models that are representative of mainstream methods of estimating energy consumption and can be easily calibrated using the vehicle CAN bus data.

First, Yao's BEV energy consumption model is a multivariate regression model consisting of linear, quadratic, and cubic combinations of speed and acceleration (Yao et al. 2014). The model was developed based on chassis dynamometer experiment data. The model parameters are calibrated for different vehicle modes—acceleration, deceleration, cruising, and idling. Yao's model is described as follows:

$$ECR = \begin{cases} \sum_{i=0}^{3}\sum_{j=0}^{3}(\omega_{i,j} \times v^i \times a^j) & a > 0 \\ \sum_{i=0}^{3}\sum_{j=0}^{3}(\beta_{i,j} \times v^i \times a^j) & a < 0 \\ \sum_{i=0}^{3}(\theta_i \times v^i) & a = 0, v \neq 0 \\ \overline{ecr} & a = 0, v = 0 \end{cases} \quad (37)$$

where
$ECR$ is energy consumption rate (W)
$\omega_{i,j}$, $\beta_{i,j}$, $\theta_i$ are coefficients
$\overline{ecr}$ is average energy consumption (W) in idling mode

Second, Yang et al. (2014) proposed a BEV energy consumption model, considering vehicle-specific power and auxiliary load, as well as the energy efficiency of regenerative braking. When instantaneous acceleration $a \geq 0$, the energy consumption rate is calculated as

$$ECR = \frac{m}{\eta_{te}\eta_e} VSP + P_{accessory}, \ a \geq 0 \quad (38)$$

where
$m$ is vehicle mass (kg)
$\eta_{te}$ is BEV's transmission efficiency
$\eta_e$ is driving efficiency of battery
$VSP$ is vehicle specific power (W/kg)
$P_{accessory}$ is the electricity consumed by accessories (W)

When the vehicle decelerates, a portion of kinetic energy is recovered and restored in batteries due to the regenerative braking feature of motors. The regenerative braking factor $\eta$ in Equation 38 indicates the percentage of braking energy that can be recovered, which varies with speed. Note that in practice, $\eta$ is influenced by many factors, such as speed, deceleration, and braking force. In Yang et al.'s model, $\eta$ is defined as a function of speed, as in Equation 39.

$$ECR = \eta m \eta_{te} \eta_m VSP + P_{accessory} \quad a < 0 \tag{39}$$

$$\eta = \begin{cases} 0.5 \times \frac{v}{5}, & v < 5 \\ 0.5 + 0.3 \times \frac{v-5}{20}, & v \geq 5 \end{cases} \tag{40}$$

where
$\eta$ is regenerative braking factor
$\eta_m$ is motor efficiency

*Proposed BEV Energy Consumption Model*

Most of the existing electricity consumption models were developed based on the data collected in heterogeneous driving conditions. For example, Yao et al. (2014) and Fiori et al. (2016) used data collected from chassis dynamometer experiments, and Zhang and Yao (2015) collected data in low-speed urban traffic conditions. Alves et al. (2016) collected data under constant ambient temperature. By using real-world driving data collected on urban roads and highways over an extended time period, an electricity consumption model that considers vehicle-specific power, regenerative braking, auxiliary load, and ambient temperature is proposed to estimate BEV on-road energy consumption.

VSP provides an estimate of the battery output power per mass unit for overcoming the resistance encountered by a BEV (Alves et al. 2016, Boroujeni and Frey 2014). It is calculated using vehicle dynamics in Equation 41. Energy consumption is heterogeneous at different VSP levels (Alves et al. 2016). Negative values of VSP indicate that due to regenerative braking, some electricity is converted from kinetic energy and restored in the batteries. Therefore, the proposed energy consumption model is calibrated based on VSP levels (>0, =0, or <0) to account for regenerative braking.

$$VSP = v(1.1a + C_{rr}) + C_{aero} v^3 \tag{41}$$

where
$C_{rr}$ is rolling resistance coefficient (N/kg)
$C_{aero}$ is aerodynamics drag coefficient (N $s^2/m^2$ kg)

Auxiliary systems, especially heating and air conditioning systems, consume considerable electricity (Fiori et al. 2016, Liu et al. 2017). The relationship between average auxiliary load and ambient temperature for each trip is illustrated in Figure 3.

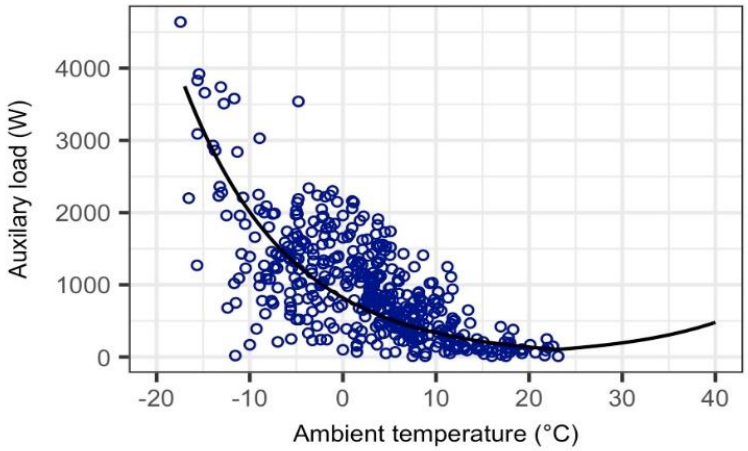


**Figure 3. Relationship between auxiliary load and ambient temperatures**

The data were collected using an OBD-II logger and a GPS device installed on a passenger BEV (2013 Nissan Leaf) for six months in real-world driving conditions. Since the data were collected from November 2016 to April 2017 in Iowa, the ambient temperature range only covers -17 °C to 23 °C. Thus, part of the curve (i.e., ambient temperature from -17 °C to 23 °C) is calibrated using the data. The R-squared is 0.46. $c_0$ and $c_1$ are 6.71 and -0.0894, respectively. Yuksel and Michalek (2015), Wang et al. (2017), and Liu et al. (2017(a)) explored the U-shaped relationship between BEV energy consumption and ambient temperature, where the energy consumption is lowest at 20 °C ~ 25 °C and increases as the temperature becomes colder or hotter, with similar trends. In this study, a symmetric equation is assumed to estimate the auxiliary load from 23 °C to 40 °C, as shown in Equation 42.

$$\ln P_{aux} = \begin{cases} c_0 + c_1 t, & if -17 \le t \le 23 \\ c_0 + c_1(46 - t), & if\ 23 < t \le 40 \end{cases} \quad (42)$$

where
$P_{aux}$ is vehicle auxiliary load (W)
$t$ is ambient temperature (°C)
$c_0, c_1$ are coefficients

Considering the VSP and auxiliary load, a hybrid linear regression model is proposed to estimate BEV electricity consumption.

$$ECR = h_0 + h_1 VSP + h_2 P_{aux} \quad (43)$$

where $h_0$, $h_1$, $h_2$ are coefficients.

The model parameters are calibrated at different VSP levels to account for regenerative braking. Moreover, unlike internal combustion engine vehicles that are more fuel efficient on highways, BEVs driving at high speeds consume more electricity per distance unit than at low speeds (Alves et al. 2016, Fiori et al. 2016, Yang et al. 2013, Wager et al. 2016). Therefore, the model parameters are calibrated at different instantaneous speed levels. The threshold of 12.5 m/s (or 45 km/h) is used to separate high-speed driving from low-speed driving.

*Calibration and Validation of the Proposed BEV Energy Consumption Model*

The parameters of the proposed BEV energy consumption model are calibrated using the vehicle data collected from a 2013 Nissan Leaf. For this vehicle, $C_{rr}$ equals 0.0981 N/kg and $C_{aero}$ equals 0.0002 N $s^2/m^2$ kg (Faria et al. 2012, Fiori et al. 2016, Wager et al. 2016). The vehicle was primarily used on urban roads and major highways. The data collected include timestamp, GPS location, vehicle speed, ambient temperature, battery current and voltage, and battery SOC. Energy consumption is the product of battery voltage and current. Acceleration is the derivative of vehicle speeds. During the six-month data collection period, 512 trips were recorded. The calibrated model parameters are listed in Table 4.

**Table 4. Parameters of the electricity consumption model**

| *VSP* | *v* | $h_0$ | $h_1$ | $h_2$ | $c_0$ | $c_1$ |
|---|---|---|---|---|---|---|
| >0 | <12.5 | 3.22E+03 | 1.16E+03 | 2.15E+00 | 6.71E+00 | -8.94E-02 |
| | ≥12.5 | 8.43E+03 | 7.57E+02 | 2.60E+00 | | |
| =0 | <12.5 | 6.10E+02 | — | 1.19E+00 | | |
| | ≥12.5 | — | — | — | | |
| <0 | <12.5 | 7.20E+02 | 5.58E+02 | 2.10E+00 | | |
| | ≥12.5 | 8.12E+03 | 5.94E+02 | 2.57E+00 | | |

Moreover, Yao's model and Yang et al.'s model are calibrated and validated using the same dataset. The trip-level energy consumptions estimated by the proposed model, Yao's model, and the Yang et al.'s model are compared with the actual energy consumption for the same trip. As shown in Figure 4, the proposed model can estimate trip-level energy consumptions fairly close to the actual values and outperforms Yao's and Yang et al.'s models.

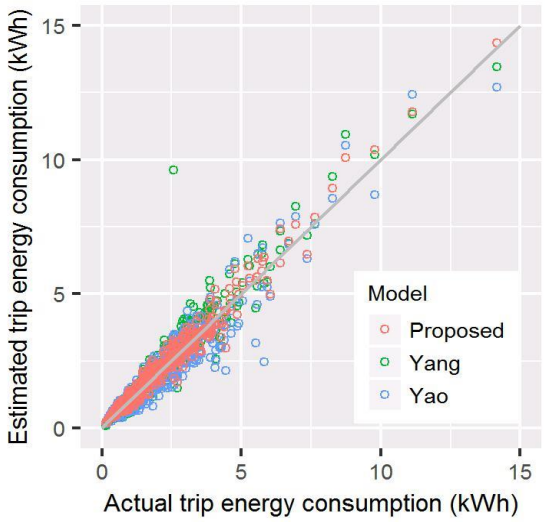


**Figure 4. Validation of the electricity consumption models**

The mean absolute percentage error and root mean square error are calculated and compared for these three models, as listed in Table 5.

**Table 5. Validation metrics for BEV electricity consumption model**

| Electricity consumption models | MAPE | RMSE |
|---|---|---|
| Proposed model | 13.3% | 0.296 kWh |
| Yao's model | 19.5% | 0.495 kWh |
| Yang et al.'s model | 16.7% | 0.511 kWh |

$$MAPE = \frac{1}{p}\sum_{i=1}^{p}\left|\frac{EC_{a,i}-EC_{e,i}}{EC_{a,i}}\right| \times 100\% \quad (44)$$

$$RMSE = \sqrt{\frac{\sum_{i=1}^{n}(EC_{a,i}-EC_{e,i})^2}{p}} \quad (45)$$

where
$EC_{e,i}$ is the estimated energy consumption of trip $i$ (kWh)
$EC_{a,i}$ is the actual energy consumption of trip $i$ (kWh)
$p$ is the total number of trips in the dataset (i.e., 512)

Among these models, the proposed model has the lowest MAPE and RMSE. Consequently, the proposed model is used to estimate electricity consumption of BEVs.

## ENERGY EFFICIENCY OF CAVS IN A MIXED FLEET

The numerical experiments are performed by simulating a traffic stream with 1,000 vehicles on a 7.45-mile long single lane road. As the platoon size on urban arterials usually ranges from 14 to 81 vehicles (Baas and Serge 1988, Bie et al. 2013) when the number of lane is less than 4, the traffic stream is divided into platoons with a size of 14 to 81 vehicles. The lead vehicle of each platoon is assumed to follow the Urban Dynamometer Driving Schedule (UDDS) (EPA 2017), as shown in Figure 5.

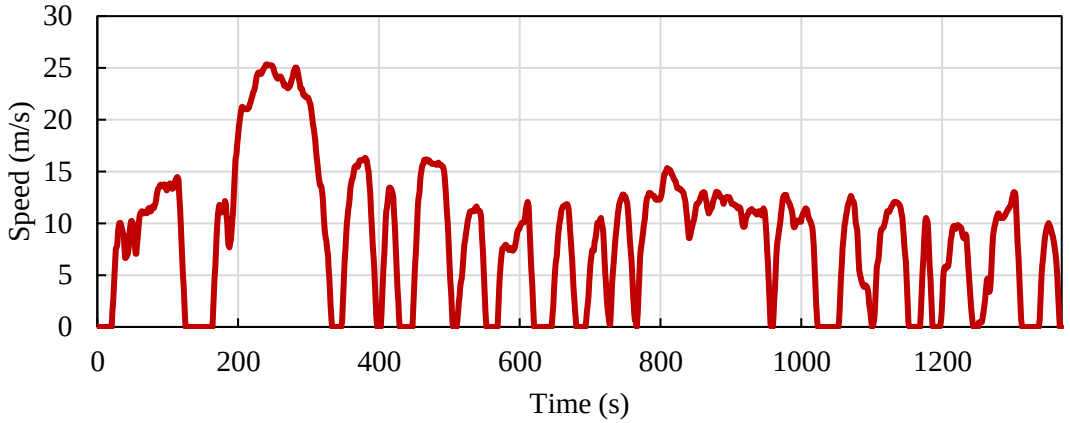


**Figure 5. Urban Dynamometer Driving Schedule (UDDS)**

In each platoon, the initial spacing and time headway are set as the desired spacing and desired time headway, respectively. Various scenarios are simulated, considering traffic streams with all CAVs, all manually driven vehicles, or a mix of the two. In the case of mixed traffic, different market penetrations of CAVs are simulated. The car following behavior of manually driven vehicles is assumed to follow the IDM. For gasoline CAVs, different adaptive cruise control strategies are tested, including IDM-ACC, Nissan-ACC, and the Eco-SDM. Moreover, considering traffic streams with all e-CAVs, all human-driven vehicles, or a mix of the two. In the case of a mixed traffic stream, different market penetrations of e-CAVs are simulated. The car-following behavior of human-driven vehicles is assumed to follow the IDM. For e-CAVs, different adaptive cruise control strategies are simulated, including IDM-ACC, Nissan-ACC, CACC, and the $E^3$DM.

### Energy Efficiency of Gasoline CAVs

To demonstrate the impact of CAVs on individual vehicle and platoon-level fuel consumption, 1 platoon consisting of 16 vehicles is examined. Figure 6 compares the fuel consumption of each following vehicle in the traffic stream assuming all manually driven vehicles (i.e., manual) and all CAVs (i.e., IDM-ACC, Nissan-ACC, and the Eco-SDM).

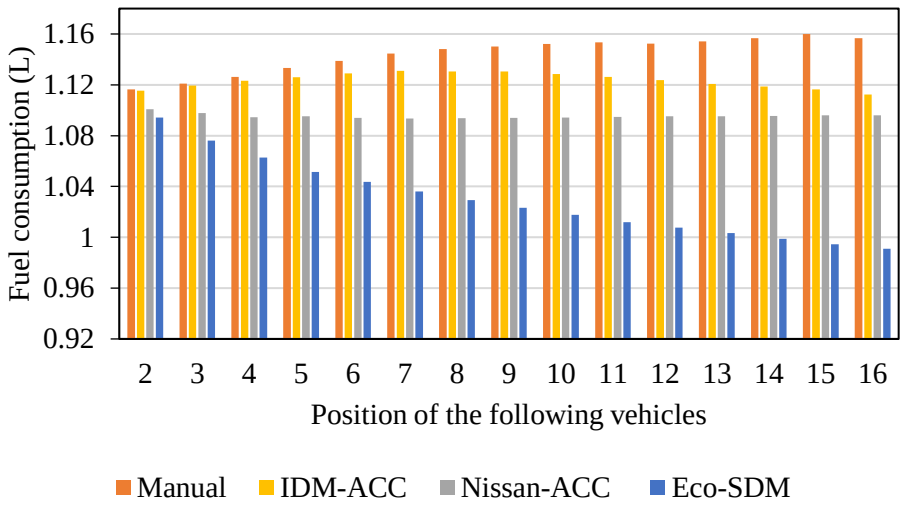


**Figure 6. Fuel consumption comparison assuming all manually driven vehicles or all CAVs**

In the homogeneous traffic stream, the CAVs consume less fuel than the manually driven vehicles. In addition, the Eco-SDM outperforms IDM-ACC and Nissan-ACC in terms of fuel economy. The Eco-SDM reduces fuel consumption of the entire fleet by approximately 10%, compared to the all-manual case.

Figure 7 compares the travel times of different car following strategies.

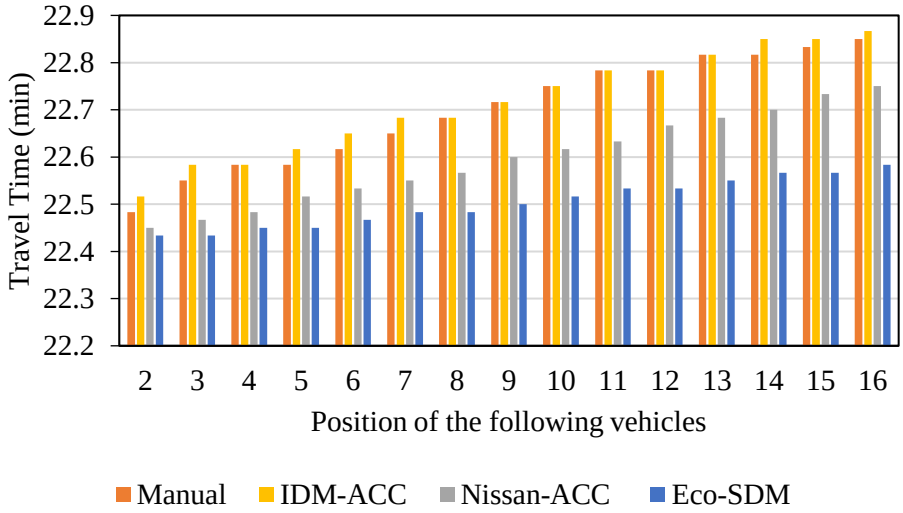


**Figure 7. Travel time comparison assuming all manually driven vehicles or all CAVs**

IDM-ACC slightly increases travel time compared to the manually driven fleet. The Eco-SDM results in the least travel time among all the control strategies.

The reason for the better performance of the Eco-SDM is that it provides smoother deceleration and acceleration compared to Nissan-ACC and IDM-ACC. As shown in Figure 8, with ACC, CAVs toward the end of the platoon tend to reach smooth deceleration and acceleration. The Eco-SDM stabilizes the string much faster than Nissan-ACC or IDM-ACC.

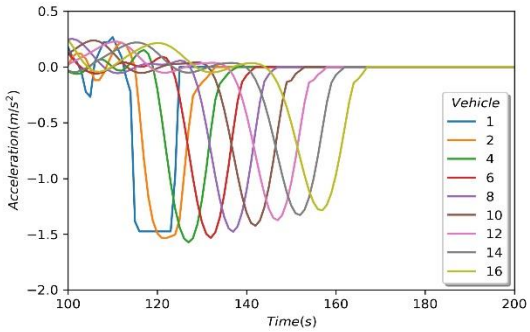


**(a) Nissan-ACC**

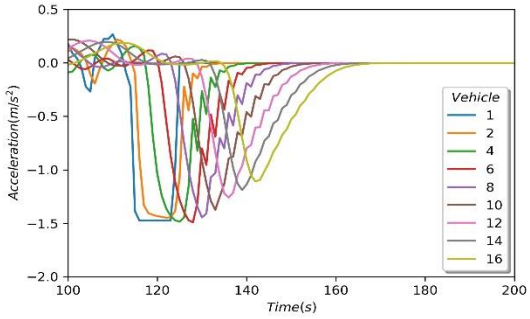


**(b) IDM-ACC**

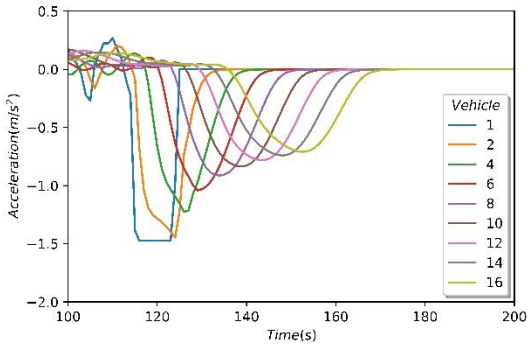


**(c) Eco-SDM**

**Figure 8. Acceleration profiles of different ACC strategies**

Moreover, a mixed platoon with 1 CAV and 15 manually driven vehicles is selected to examine the impact of CAV location on the total fuel consumption of the fleet. The location of the CAV varies from immediately following the manually driven vehicle to the end of the vehicle set. As shown in Figure 9, all ACC strategies reduce fleet-level fuel consumption with only one equipped vehicle.

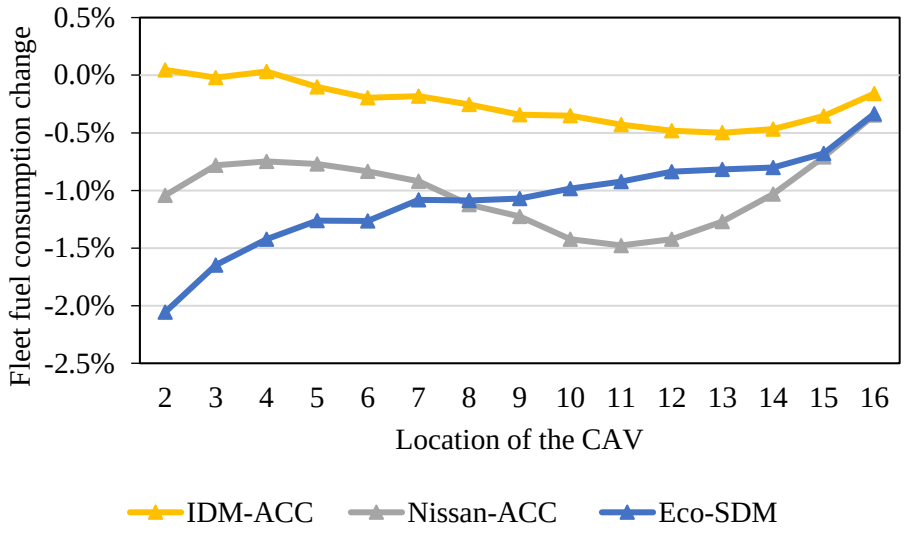


**Figure 9. Impact of CAV location on total fuel consumption**

For the Eco-SDM, a CAV toward the front of the platoon has larger impacts on the fleet-level fuel efficiency, compared to the case when the CAV is toward the end of the platoon. One Eco-SDM CAV may result in up to 2% reduction in total fuel consumption if placed at the front of the platoon. However, with Nissan-ACC and IDM-ACC, there is no obvious relationship between the location of the CAV and fuel consumption.

Furthermore, the impact of different market penetration of CAVs on fuel consumption is examined by simulating traffic streams with mixed CAVs and manually driven vehicles. By changing CAV market penetration and the locations of CAVs in the platoon, 500 simulations were run for each ACC model. The mean fuel consumption reduction of the entire fleet, compared to the all manually driven vehicle scenario, is shown in Figure 10.

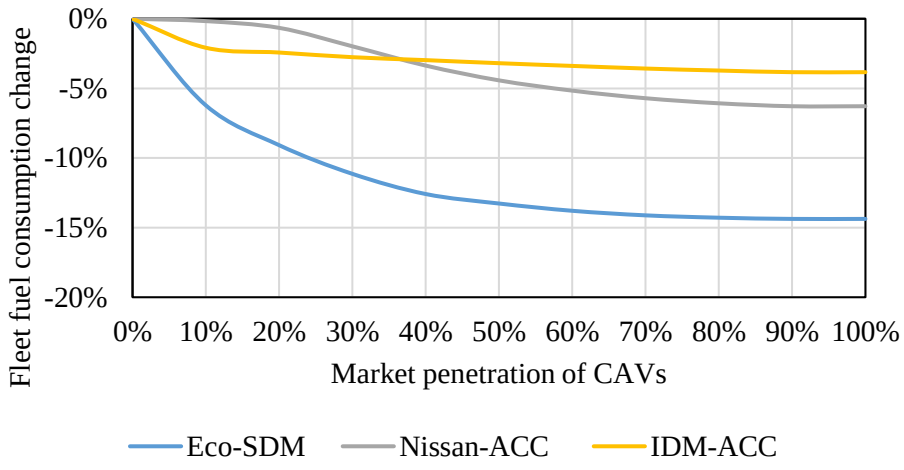


**Figure 10. Impact of CAV market penetration on total fuel consumption**

Generally, the higher market penetration of CAVs results in better fuel efficiency of the fleet. With the Eco-SDM, the marginal improvement in fuel efficiency decreases when the market penetration of CAVs exceeds 30%.

**Energy Efficiency of Electric CAVs**

*Homogenous Traffic Stream*

To demonstrate the impact of e-CAVs on individual vehicle and platoon-level energy consumption, 1 platoon consisting of 16 BEVs was examined. Figure 11 compares the energy consumption of each following vehicle in the traffic streams with all human-driven vehicles (i.e., manual) or all CAVs (i.e., IDM-ACC, Nissan-ACC, CACC, and the E$^3$DM).

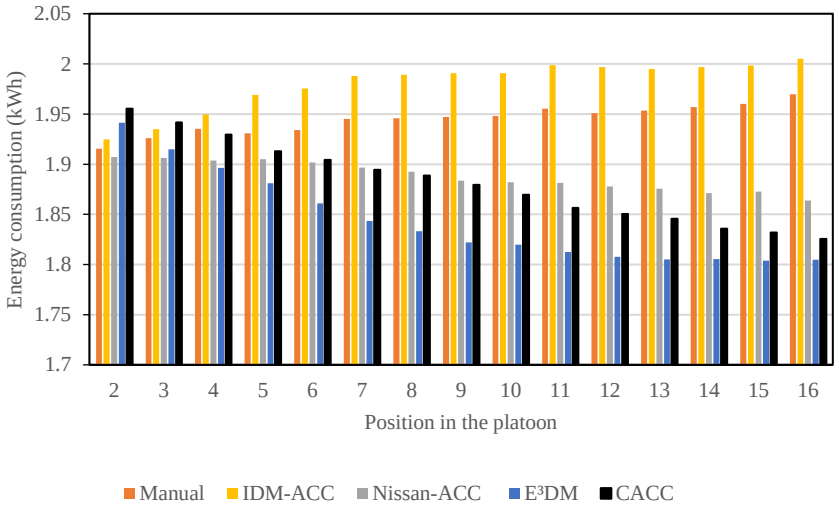


**Figure 11. Energy consumption comparison assuming all manually driven vehicles or all e-CAVs**

In the homogeneous traffic stream, the e-CAVs equipped with the E$^3$DM and Nissan-ACC consume less energy than the manually driven vehicles. IDM-ACC-equipped e-CAVs, however, consume more energy than the manually driven vehicles. The reason is that IDM-ACC provides smoother deceleration, which may reduce the regenerative energy of BEVs. The E$^3$DM outperforms IDM-ACC, CACC, and Nissan-ACC in terms of energy consumption. The E$^3$DM reduces energy consumption of the entire platoon by approximately 5.2%, compared to the all-manual case. Moreover, the average travel times of the IDM, IDM-ACC, Nissan-ACC, CACC, and the E$^3$DM are 22.7, 22.6, 22.7, 22.5, and 22.8 minutes, respectively. The E$^3$DM slightly increases travel time compared to the manually driven fleet. However, the increase in travel time is not significant.

The reason for the better performance of the E$^3$DM is its application of small decelerations for long durations instead of large decelerations for short durations, as shown in Figure 12.

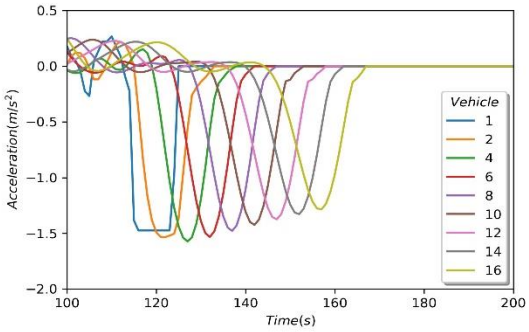


**(a) Nissan-ACC**

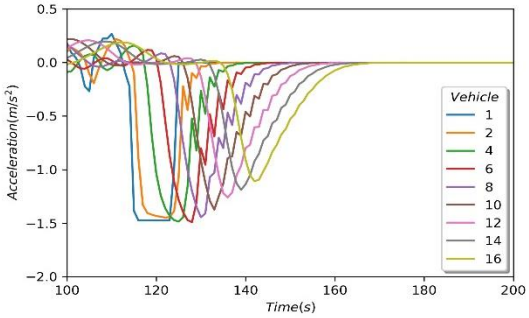


**(b) IDM-ACC**

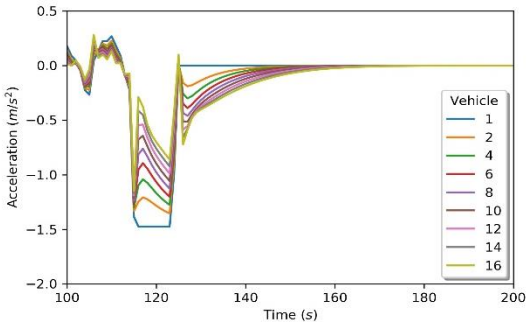


**(c) CACC**

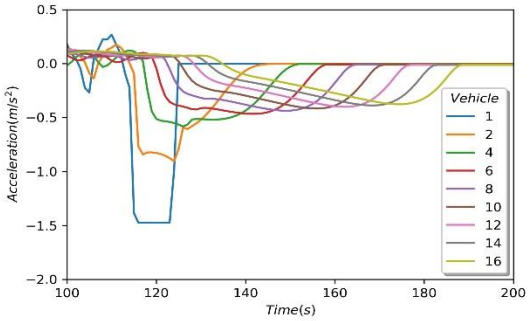


**(d) E$^3$DM**

**Figure 12. Acceleration profiles of different ACC strategies**

Thus, the E$^3$DM is able to keep high regenerative braking efficiency for a longer duration compared to Nissan-ACC, CACC, and IDM-ACC. In addition, the E$^3$DM also provides smoother deceleration and acceleration compared to Nissan-ACC and IDM-ACC. As shown in Figure 12,

with ACC and CACC, e-CAVs toward the end of the platoon tend to reach smooth deceleration and acceleration. The E$^3$DM stabilizes the string much faster than Nissan-ACC or IDM-ACC.

*Mixed Traffic Stream*

To examine the impact of e-CAV location on the total energy consumption, a platoon with 1 e-CAV and 15 manually driven BEVs was selected. The location of the e-CAV varies from immediately following the manually driven vehicle to the end of the platoon. As shown in Figure 13, the Nissan-ACC and E$^3$DM strategies reduce fleet-level energy consumption with only one equipped vehicle.

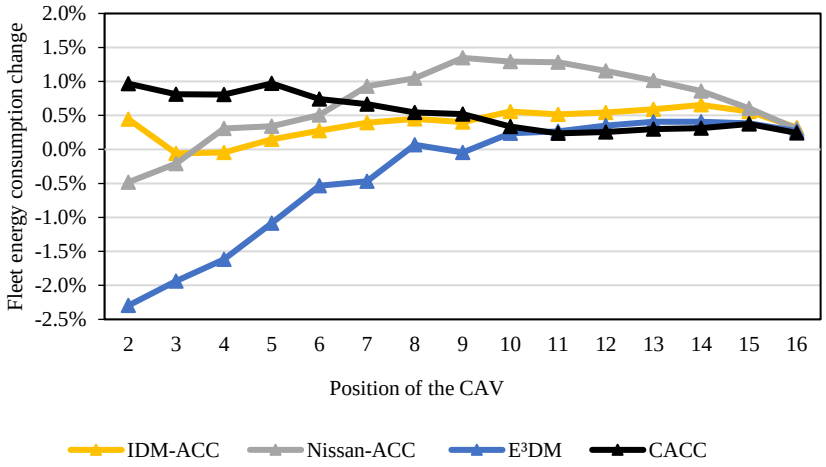


**Figure 13. Impact of e-CAV location on total energy consumption**

For the E$^3$DM, an e-CAV toward the front of the platoon has more significant impacts on the fleet-level energy efficiency, compared to the case when the e-CAV is toward the end of the platoon. One E$^3$DM-equipped e-CAV may result in up to 2.4% reduction in total energy consumption if placed at the front of the platoon. However, with Nissan-ACC and IDM-ACC, there is no obvious relationship between the location of the e-CAV and total energy consumption.

Furthermore, the impact of different market penetrations of e-CAVs on energy consumption was examined by simulating traffic streams with mixed e-CAVs and manually driven vehicles. Two scenarios were considered.

First, to examine the impact of e-CAV market penetration on total energy consumption, 500 simulations were generated for each ACC strategy and each market penetration rate, by randomly assigning e-CAV locations in the platoon. The mean energy consumption reduction of the entire fleet, compared to the all manually driven BEV scenario, is shown in Figure 14.

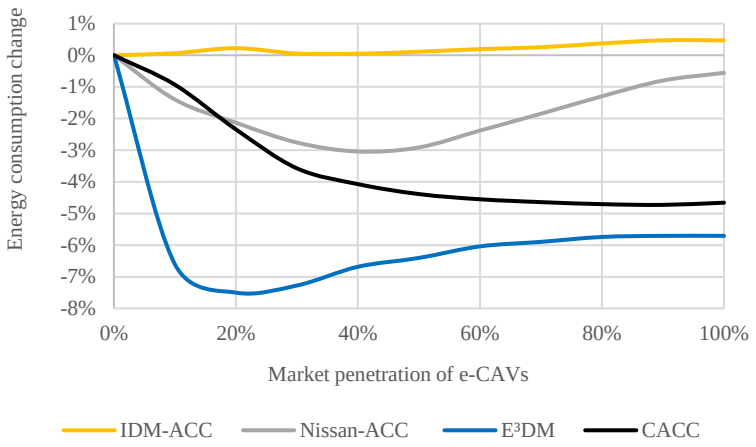


**Figure 14. Impact of e-CAV market penetration on total energy consumption**

Higher market penetration of e-CAVs may not result in better energy efficiency of the entire fleet. With the E$^3$DM, the highest fleet-level energy efficiency is achieved when the market penetration of e-CAVs is 20%. A higher percentage of e-CAVs in the traffic stream results in faster string stabilization, which decreases the regenerative energy.

Second, to examine the synergistic effect of CAV and BEV technologies, mixed traffic streams with e-CAVs, manually driven BEVs (m-BEVs), and manually driven internal-combustion engine vehicles (m-ICEVs) were simulated. The fuel consumption of an m-ICEV was computed by applying the calibrated VT-Micro model and then converting the results to electricity (DOE 2017). The electricity consumption of e-CAVs and m-BEVs was computed using the proposed BEV energy consumption model. The impact of different market shares of e-CAVs, m-BEVs, and m-ICEVs on energy consumption reduction of the entire fleet was investigated, as shown in Figure 15.

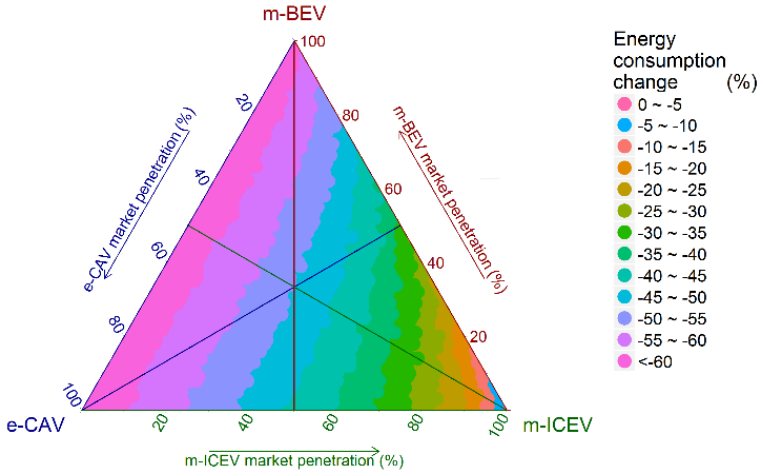


**Figure 15. Impact of different market penetration of e-CAV, human-driven BEV, and manually driven ICEV on total energy consumption**

The marginal improvement in energy efficiency decreases when the market penetration of BEVs, including e-CAVs and m-BEVs, exceed 20%. Moreover, the larger the market penetration ratio of e-CAVs to m-BEVs is, the faster the marginal improvement in energy efficiency reaches the turning point.

## CONCLUSIONS

First, this report presented an ecological smart driver model (Eco-SDM) for adaptive cruise control (ACC) of gasoline CAVs in a mixed traffic stream. Considering the location of a CAV relative to other CAVs and manually driven vehicles, the Eco-SDM adjusts the desired spacing between the following and leading vehicle to provide smooth deceleration and acceleration. The impact of the Eco-SDM on fuel consumption was investigated, using the fuel consumption model calibrated based on on-road vehicle operational data.

The key findings regarding the energy efficiency of gasoline CAVs in a mixed fleet were as follows:

- By simulating single-lane vehicle dynamics in a platoon with different percentages of CAVs, the results show that CAVs are generally more fuel efficient than manually driven vehicles.

- The Eco-SDM outperforms IDM-ACC and Nissan-ACC in terms of fuel efficiency and travel time.

- Higher market penetration of CAVs results in better fuel efficiency of the fleet. When the market penetration of the Eco-SDM-equipped CAVs exceeds 30%, the marginal improvement of fuel efficiency decreases.

- One Eco-SDM CAV may result in up to 2% reduction in total fuel consumption if placed at the front of the platoon.

Second, an energy-efficient electric driving model, the $E^3$DM, was proposed for ACC of e-CAVs in traffic streams mixed with human-driven vehicles. Considering the location of an e-CAV relative to other e-CAVs and human-driven vehicles, the $E^3$DM is able to maintain high efficiency of regenerative braking and provide smooth deceleration and acceleration by adjusting the spacing between leading and following vehicles. Moreover, a power-based energy consumption model was proposed to estimate the on-road energy consumption for BEVs. Using the proposed BEV energy consumption model, the impact of the $E^3$DM on energy consumption of individual vehicles and the entire fleet was investigated.

The key findings about the energy efficiency of e-CAVs in a mixed fleet were as follows:

- By simulating single-lane vehicle dynamics in a platoon with different percentages of e-CAVs, the results show that e-CAVs equipped with the $E^3$DM and Nissan-ACC consume less energy than human-driven vehicles.

- The $E^3$DM outperforms IDM-ACC, CACC, and Nissan-ACC in terms of energy efficiency.

- Higher market penetration of e-CAVs may not result in better energy efficiency of the entire fleet. With the $E^3$DM, the highest energy efficiency is achieved when the market penetration of e-CAVs is 20%. This is because more e-CAVs in the traffic stream results in faster string stabilization and decreases the regenerative energy.

- Considering mixed traffic streams with BEVs (e-CAVs and m-BEVs) and internal combustion engine vehicles (m-ICEVs), the marginal improvement in energy efficiency decreases when the market penetration of BEVs, including e-CAVs and m-BEVs, exceeds 20%.

- The larger the market penetration ratio of e-CAVs to m-BEVs is, the faster the marginal improvement in energy efficiency reaches the turning point.

**Study Limitations and Recommendations for Additional Research**

This study has the following limitations. First, lane-changing behavior is ignored. An energy-efficient lane-changing strategy should be designed for CAVs and implemented in tandem with the Eco-SDM and $E^3$DM to simulate real-world driving behavior. Second, since the lead vehicle in each platoon is assumed to follow UDDS, the simulation is not able to represent different traffic congestion levels. In the future, different traffic states should be simulated to investigate the impact of the Eco-SDM and $E^3$DM under different congestion levels. Third, the communication delay and sensor failure are ignored in this study. The impact of these factors on the performance of CAVs will be investigated in the future.

## REFERENCES


Ahn, K., H. Rakha, A. Trani, and M. Van Aerde. 2002. Estimating vehicle fuel consumption and emissions based on instantaneous speed and acceleration levels. *Journal of Transportation Engineering*, Vol. 128, No. 2, pp. 182–190.

Ahn, K., H. Rakha, and S. Park. 2013. Ecodrive application: Algorithmic development and preliminary testing. *Transportation Research Record: Journal of the Transportation Research Board*, No. 2341, pp.1–11.

Akhegaonkar, S., L. Nouvelière, S. Glaser, and F. Holzmann. 2016. Smart and Green ACC: Energy and Safety Optimization Strategies for EVs. *IEEE Transactions on Systems, Man, and Cybernetics: Systems*, Vol. 48, No. 1, pp. 142–153.

Alves, J., P. C. Baptista, G. A. Gonçalves, and G. O. Duarte. 2016. Indirect methodologies to estimate energy use in vehicles: Application to battery electric vehicles. *Energy Conversion and Management*, Vol. 124, pp. 116–129.

Baas, K. G. and L. Serge. 1988. Analysis of platoon dispersion with respect to traffic volume. *Transportation Research Record: Journal of the Transportation Research Board*, No. 1194, pp. 64–76.

Bie, Y., Z. Liu, D. Ma, and D. Wang. 2013. Calibration of platoon dispersion parameter considering the impact of the number of lanes. *Journal of Transportation Engineering*, Vol. 139, No. 2, pp. 200–207.

Boroujeni, B. Y. and H. C. Frey. 2014. Road grade quantification based on global positioning system data obtained from real-world vehicle fuel use and emissions measurements. *Atmospheric Environment*, Vol. 85, pp. 179–186.

Chen, Y. and J. Wang. 2014. Design and experimental evaluations on energy efficient control allocation methods for overactuated electric vehicles: Longitudinal motion case. *IEEE/ASME Transactions on Mechatronics*, Vol. 19, No. 2, pp. 538–548.

Chen, Y., X. Li, C. Wiet, and J. Wang. 2014. Energy management and driving strategy for in-wheel motor electric ground vehicles with terrain profile preview. *IEEE Transactions on Industrial Informatics*, Vol. 10, No. 3, pp. 1938–1947.

Davis, L. C. 2004. Effect of adaptive cruise control systems on traffic flow. *Physical Review E*: *Statistical, Nonlinear and Soft Matter Physics*, Vol. 69, No. 6, pp. 066110-1–066110-8.

Davis, L. C. 2017. Dynamic origin-to-destination routing of wirelessly connected, autonomous vehicles on a congested network. *Physica A: Statistical Mechanics and its Applications*, Vol. 478, pp. 93–102.

De Vlieger, I. 1997. On board emission and fuel consumption measurement campaign on petrol-driven passenger cars. *Atmospheric Environment*, Vol. 31, No. 22, pp. 3753–3761.

De Vlieger, I., D. De Keukeleere, and J. G. Kretzschmar. 2000. Environmental effects of driving behaviour and congestion related to passenger cars. *Atmospheric Environment*, Vol. 34, No. 27, pp. 4649–4655.

Dey, K. C., L. Yan, X. Wang, Y. Wang, H. Shen, M. Chowdhury, L. Yu, C. Qiu, and V. Soundararaj. 2016. A review of communication, driver characteristics, and controls aspects of cooperative adaptive cruise control (CACC). *IEEE Transactions on Intelligent Transportation Systems*, Vol. 17, No. 2, pp. 491–509.

DOE. 2017. *Alternative Compliance*. U.S. Department of Energy, Washington, DC. https://epact.energy.gov/pdfs/alt_compliance_guide.pdf. Last accessed December 2017.

Enang, W. and C. Bannister. 2017. Modelling and control of hybrid electric vehicles (A comprehensive review). *Renewable and Sustainable Energy Reviews*, Vol. 74, pp. 1210–1239.

EPA. 2016. *Light-Duty Automotive Technology, Carbon Dioxide Emissions, and Fuel Economy Trends: 1975 through 2016*. U.S. Environmental Protection Agency, Washington, DC. https://nepis.epa.gov/Exe/ZyPDF.cgi?Dockey=P100PKK8.pdf. Last accessed April 2018.

EPA. 2017. *Dynamometer Drive Schedules*. U.S. Environmental Protection Agency, Washington, DC. https://www.epa.gov/vehicle-and-fuel-emissions-testing/dynamometer-drive-schedules. Last accessed July 2017.

Fancher, P., H. Peng, Z. Bareket, C. Assaf, and R. Ervin. 2002. Evaluating the influences of adaptive cruise control systems on the longitudinal dynamics of strings of highway vehicles. *Vehicle System Dynamics*, Vol. 37, No. 1, pp. 125–136.

Faria, R., P. Moura, J. Delgado, and A. T. De Almeida. 2012. A sustainability assessment of electric vehicles as a personal mobility system. *Energy Conversion and Management*, Vol. 61, pp. 19–30.

Fiori, C., K. Ahn, and H. A. Rakha. 2016. Power-based electric vehicle energy consumption model: Model development and validation. *Applied Energy*, Vol. 168, pp. 257–268.

Genikomsakis, K. N. and G. Mitrentsis. 2017. A computationally efficient simulation model for estimating energy consumption of electric vehicles in the context of route planning applications. *Transportation Research Part D: Transport and Environment*, Vol. 50, pp. 98–118.

Gipps, P. G. 1981. A behavioural car-following model for computer simulation. *Transportation Research Part B: Methodological*, Vol. 15, No. 2, pp. 105–111.

Huang, X. and J. Wang. 2012. Model predictive regenerative braking control for lightweight electric vehicles with in-wheel motors. *Proceedings of the Institution of Mechanical Engineers, Part D: Journal of Automobile Engineering*, Vol. 226, No. 9, pp. 1220–1232.

Ioannou, P. A. and M. Stefanovic. 2005. Evaluation of ACC vehicles in mixed traffic: Lane change effects and sensitivity analysis. *IEEE Transactions on Intelligent Transportation Systems*, Vol. 6, No. 1, pp. 79–89.

Jiang, R., M. Hu, B. Jia, R. Wang, and Q. Wu. 2007. Phase transition in a mixture of adaptive cruise control vehicles and manual vehicles. *The European Physical Journal B*, Vol. 58, No. 2, pp. 197–206.

Jung, J. and R. Jayakrishnan. 2012. High-coverage point-to-point transit: electric vehicle operations. *Transportation Research Record: Journal of the Transportation Research Board*, No. 2287, pp. 44–53.

Kamal, M. A. S., M. Mukai, J. Murata, and T. Kawabe. 2011. Ecological vehicle control on roads with up-down slopes. *IEEE Transactions on Intelligent Transportation Systems*, Vol. 12, No. 3, pp. 783–794.

Kesting, A., M. Treiber, and D. Helbing. 2010. Enhanced intelligent driver model to access the impact of driving strategies on traffic capacity. *Philosophical Transactions of the Royal Society of London A: Mathematical, Physical and Engineering Sciences*, Vol. 368, No. 1928, pp. 4585–4605.

Kesting, A., M. Treiber, M. Schönhof, and D. Helbing. 2008. Adaptive cruise control design for active congestion avoidance. *Transportation Research Part C: Emerging Technologies*, Vol. 16, No. 6, pp. 668–683.

Kikuchi, S., N. Uno, and M. Tanaka. 2003. Impacts of shorter perception-reaction time of adapted cruise controlled vehicles on traffic flow and safety. *Journal of Transportation Engineering*, Vol. 129, No. 2, pp. 146–154.

Li, S. E., Z. Jia, K. Li, and B. Cheng. 2015a. Fast online computation of a model predictive controller and its application to fuel economy-oriented adaptive cruise control. *IEEE Transactions on Intelligent Transportation Systems*, Vol. 16, No. 3, pp. 1199–1209.

Li, S. E., K. Deng, Y. Zheng, and H. Peng. 2015b. Effect of Pulse-and-Glide strategy on traffic flow for a platoon of mixed automated and manually driven vehicles. *Computer-Aided Civil and Infrastructure Engineering*, Vol. 30, No. 11, pp. 892–905.

Liang, C. and H. Peng. 2000. String stability analysis of adaptive cruise controlled vehicles. *JSME International Journal Series C, Mechanical Systems, Machine Elements and Manufacturing*, Vol. 13, No. 3, pp. 671–677.

Liu, K., J. Wang, T. Yamamoto, and T. Morikawa. 2017(a). Exploring the interactive effects of ambient temperature and vehicle auxiliary loads on electric vehicle energy consumption. *Applied Energy*, In Press.

Liu, K., T. Yamamoto, and T. Morikawa. 2017(b). Impact of road gradient on energy consumption of electric vehicles. *Transportation Research Part D: Transport and Environment*, Vol. 54, pp. 74–81.

Lu, C., L. Hu, and J. Dong. 2018. Ecological adaptive cruise control in a traffic stream with mixed autonomous and manually driven vehicles. Paper presented at the Transportation Research Board 97th Annual Meeting, January 7–11, Washington, DC.

Luo, Y., T. Chen, S. Zhang, and K. Li. 2015. Intelligent hybrid electric vehicle ACC with coordinated control of tracking ability, fuel economy, and ride comfort. *IEEE Transactions on Intelligent Transportation Systems*, Vol. 16, No. 4, pp. 2303–2308.

Mersky, A. C. and C. Samaras. 2016. Fuel economy testing of autonomous vehicles. *Transportation Research Part C: Emerging Technologies*, Vol. 65, pp. 31–48.

Milanés, V. and S. E. Shladover. 2014. Modeling cooperative and autonomous adaptive cruise control dynamic responses using experimental data. *Transportation Research Part C: Emerging Technologies*, Vol. 48, pp. 285–300.

Newell, G. F. 1961. Nonlinear effects in the dynamics of car following. *Operations Research*, Vol. 9, No. 2, pp. 209–229.

Park, S., H. Rakha, K. Ahn, and K. Moran. 2013. Virginia Tech comprehensive power-based fuel consumption model (VT-CPFM): model validation and calibration considerations. *International Journal of Transportation Science and Technology*, Vol. 2, No. 4, pp. 317–336.

Park, S., H. Rakha, K. Ahn, K. Moran, B. Saerens, and E. Van den Bulck. 2012. Predictive ecocruise control system: model logic and preliminary testing. *Transportation Research Record: Journal of the Transportation Research Board*, No. 2270, pp. 113–123.

Rakha, H. and K. Ahn. 2004. Integration modeling framework for estimating mobile source emissions. *Journal of Transportation Engineering*, Vol. 130, No. 2, pp. 183–193.

Rakha, H. A., K. Ahn, K. Moran, B. Saerens, and E. Van Den Bulck. 2011. Virginia Tech Comprehensive Power-Based Fuel Consumption Model: Model development and testing. *Transportation Research Part D: Transport and Environment*, Vol. 16, No. 7, pp. 492–503.

Ribeiro, V., J. Rodrigues, and A. Aguiar. 2013. Mining geographic data for fuel consumption estimation. *Proceedings of the 16th International IEEE Conference on Intelligent Transportation Systems-(ITSC 2013)*, pp. 124–129.

Schwickart, T., H. Voos, J. Hadji-minaglou, M. Darouach, and A. Rosich. 2015. Design and simulation of a real-time implementable energy efficient model-predictive cruise controller for electric vehicles. *Journal of the Franklin Institute*, Vol. 352, No. 2, pp. 603–625.

Shladover, S. E., D. Su, and X-Y. Lu. 2012. Impacts of cooperative adaptive cruise control on freeway traffic flow. *Transportation Research Record: Journal of the Transportation Research Board*, No. 2324, pp. 63–70.

Talebpour, A. and H. S. Mahmassani. 2016. Influence of connected and autonomous vehicles on traffic flow stability and throughput. *Transportation Research Part C: Emerging Technologies*, Vol. 71, pp. 143–163.

Talebpour, A., H. S. Mahmassani, and S. H. Hamdar. 2011. Multiregime sequential risk-taking model of car-following behavior: Specification, calibration, and sensitivity analysis. *Transportation Research Record: Journal of the Transportation Research Board*, Vol. 2260, pp. 60–66.

Treiber, M., A. Hennecke, and D. Helbing. 2000. Congested traffic states in empirical observations and microscopic simulations. *Physical Review E*, Vol. 62, No. 2, pp. 1805–1824.

Vajedi, M. and N. L. Azad. 2016. Ecological adaptive cruise controller for plug-in hybrid electric vehicles using nonlinear model predictive control. *IEEE Transactions on Intelligent Transportation Systems*, Vol. 17, No. 1, pp. 113–122.

Van Arem, B., C. J. G. Van Driel, and R. Visser. 2006. The impact of cooperative adaptive cruise control on traffic-flow characteristics. *IEEE Transactions on Intelligent Transportation Systems*, Vol. 7, No. 4, pp. 429–436.

Van Mierlo, J., G. Maggetto, E. Van De Burgwal, and R. Gense. 2004. Driving style and traffic measures—influence on vehicle emissions and fuel consumption. *Proceedings of the Institution of Mechanical Engineers, Part D: Journal of Automobile Engineering*, Vol. 218, No. 1, pp. 43–50.

Wager, G., J. Whale, and T. Braunl. 2016. Driving electric vehicles at highway speeds: The effect of higher driving speeds on energy consumption and driving range for electric vehicles in Australia. *Renewable and Sustainable Energy Reviews*, Vol. 63, pp. 158–165.

Wang, J., K. Liu, T. Yamamoto, and T. Morikawa. 2017. Improving estimation accuracy for electric vehicle energy consumption considering the effects of ambient temperature. *Energy Procedia*, Vol. 105, pp. 2904–2909.

Wang, M., S. P. Hoogendoorn, W. Daamen, B. van Arem, B. Shyrokau, and R. Happee. 2018. Delay-compensating strategy to enhance string stability of autonomous vehicle platoons. *Transportmetrica B: Transport Dynamics*, Vol. 6, No. 3, pp. 211–229.

Wang, Z., X. M. Chen, Y. Ouyang, and M. Li. 2015. Emission mitigation via longitudinal control of intelligent vehicles in a Congested Platoon. *Computer-Aided Civil and Infrastructure Engineering*, Vol. 30, No. 6, pp. 490–506.

Wu, X., X. He, G. Yu, A. Harmandayan, and Y. Wang. 2015. Energy-optimal speed control for electric vehicles on signalized arterials. *IEEE Transactions on Intelligent Transportation Systems*, Vol. 16, No. 5, pp. 2786–2796.

Xiao, L., M. Wang, and B. van Arem. 2017 Realistic car-following models for microscopic simulation of adaptive and cooperative adaptive cruise control vehicles. *Transportation Research Record: Journal of the Transportation Research Board*, No. 2623, pp.1–9.

Yang, H., H. Rakha, and M. V. Ala. 2017. Eco-cooperative adaptive cruise control at signalized intersections considering queue effects. *IEEE Transactions on Intelligent Transportation Systems*, Vol. 18, No. 6, pp. 1575–1585.

Yang, J., J. Dong, Z. Lin, and L. Hu. 2016. Predicting market potential and environmental benefits of deploying electric taxis in Nanjing, China. *Transportation Research Part D: Transport and Environment*, Vol. 49, pp. 68–81.

Yang, S. C., C. Deng, T. Q. Tang, and Y. Qian. 2013. Electric vehicle's energy consumption of car-following models. *Nonlinear Dynamics*, Vol. 71, No. 1-2, pp. 323–329.

Yang, S. C., M. Li, Y. Lin, and T. Q. Tang. 2014. Electric vehicle's electricity consumption on a road with different slope. *Physica A: Statistical Mechanics and its Applications*, Vol. 402, pp. 41–48.

Yao, E., M. Wang, Y. Song, and Y. Zhang. 2014. Estimating energy consumption on the basis of microscopic driving parameters for electric vehicles. *Transportation Research Record: Journal of the Transportation Research Board*, Vol. 2454, pp. 84–91.

Yuan, Y., R. Jiang, M. Hu, Q. Wu, and R. Wang. 2009. Traffic flow characteristics in a mixed traffic system consisting of ACC vehicles and manual vehicles: A hybrid modelling approach. *Physica A: Statistical Mechanics and its Applications*, Vol. 388, No. 12, pp. 2483–2491.

Yuksel, T. and J. J. Michalek. 2015. Effects of regional temperature on electric vehicle efficiency, range, and emissions in the United States. *Environmental Science & Technology*, Vol. 49, No. 6, pp. 3974–3980.

Zhang, R. and E. Yao. 2015. Electric vehicles' energy consumption estimation with real driving condition data. *Transportation Research Part D: Transport and Environment*, Vol. 41, pp. 177–187.

Zhang, S., Y. Luo, J. Wang, X. Wang, and K. Li. 2017. Predictive energy management strategy for fully electric vehicles based on preceding vehicle movement. *IEEE Transactions on Intelligent Transportation Systems*, Vol. 18, No. 11, pp. 3049–3060.

**THE INSTITUTE FOR TRANSPORTATION IS THE FOCAL POINT FOR TRANSPORTATION AT IOWA STATE UNIVERSITY.**

**InTrans** centers and programs perform transportation research and provide technology transfer services for government agencies and private companies;

**InTrans** manages its own education program for transportation students and provides K-12 resources; and

**InTrans** conducts local, regional, and national transportation services and continuing education programs.


IOWA STATE UNIVERSITY

Visit www.InTrans.iastate.edu for color pdfs of this and other research reports.